N72-22133

THE PENNSYLVANIA
STATE UNIVERSITY

CASE FILE COPY

Scientific Report No. 025

Almucantar Radio Telescope Report I:
A Preliminary Study of the Capabilities of
Large Partially Steerable Paraboloidal Antennas

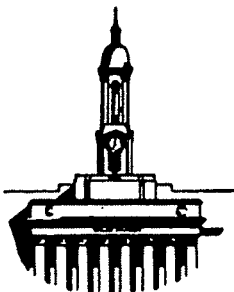by

Peter D. Usher

August 1971

RADIO ASTRONOMY OBSERVATORY

DEPARTMENT OF ASTRONOMY
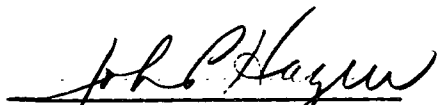
The Pennsylvania State University
College of Science

Almucantar Radio Telescope Report I:
A preliminary study of the capabilities of large partially steerable
paraboloidal antennas

Peter D. Usher

Scientific Report No. 025

Approved by:

John P. Hagen, Head
Department of Astronomy

The Pennsylvania State University

College of Science

Department of Astronomy

Table of Contents   Page

0. <u>Summary</u>

The minimum detectable flux density S_ν of a point source depends on the diameter D of a paraboloidal reflector and the integration time τ in the following way:

$$S_\nu \propto \frac{1}{D^2 \tau^{1/2}} .$$

(0.1)

Thus S_ν is more sensitive to D than to τ by a factor of 4 in the exponent. This means, that a decrease in τ, say by a factor 100, is nullified if D can be increased by a factor of only 3. Fully steerable telescopes (FST) have the capability of achieving long integration times τ, but their size D is limited by gravitational deflections. Clearly, to detect faint sources we should seek to increase D, rather then τ.

The diameter D can be increased beyond the limiting size for fully steerable telescopes by restricting the elevation steerability of the telescope in some way, and hence restricting τ. This has the consequence that a given celestial source cannot be observed at any time that it is above the horizon, but only when the earth has turned sufficiently to bring the source into the range of the telescope. To astronomers accustomed to pointing their telescope to any spot in the sky at any time, this appears to be a considerable hardship; with small telescopes, astronomers have grown accustomed to instant accessibility to all sources above the horizon. But the fact is that many routine and fundamental observing programs in radio astronomy are not hampered by restricted steerability in elevation, and indeed a few hours of patience would be a small price to pay for an incomparable minimum detectable flux and a high gain coherent beam.

Chapter 1 introduces the concept of the Almucantar radio telescope (ART) as a means of achieving a large collecting area at the expense of limited steerability

in elevation. It is shown that the almucantar telescope is the logical generalization of a fixed elevation telescope, a concept that was specifically proposed in 1963 as a solution to a gravitational deflection problem (Usher 1963).

The structure of the remaining Chapters can be grouped into four parts:

(1) Chapters 2-4 deal mainly with the geometrical consequences of limited steerability, in terms of (Chapter 2) sky coverage and Milky Way coverage, (Chapter 3) the derivation and analysis of the hour angle ΔH over which sources can be tracked by antennas of various degrees of zenith angle steerability ΔZ and (Chapter 4) the integration times and survey times for extended source distributions. The casual reader should avoid delving too deeply into these Chapters, lest he get discouraged by the details. We suggest a skim-reading with constant reference to the Figures at the back of the report which tell the whole story. These Figures show: Figure 2.1, the projection of the almucantars Z_{MAX} and Z_{MIN} (small circles of equal zenith angle) onto the celestial sphere, between which the telescope can point at any instant, with shaded areas showing the area of sky accessible in one (sidereal) day. Figures 2.2 a-d give the total sky coverage graphically for various cases of interest, Fig. 2.3 tells how to interpret the foregoing graphs, Figure 2.4 is a projection of the celestial sphere showing instantaneous positions of almucantars and the Milky Way, Fig. 2.5 is initially of marginal interest and Fig. 2.6 gives the Milky Way Sky coverage. Fig. 3.1 is a more detailed version of Fig. 2.1, defining the hour angle $\Delta H = H_{MAX} - H_{MIN}$ over which one source can be tracked, Fig. 3.2 shows how a fixed elevation telescope can track in azimuth, Figs. 3.3 a-f give ΔH (the integrating time on a point source) for varous cases, Fig. 3.4 is a

nomogram for the beamwidth $\beta = 4\lambda/\pi D$, Figs. 4.1 a-c give the integration time per unit beamwidth in a (sidereal) day for a point source that lies in a range of right ascension of 1 hour at the equator.

(2) Chapter 5 deals with radiometric capabilities of almucantar telescopes.

(3) Chapter 6 is a very preliminary account of design possibilities.

(4) Chapter 7 enumerates our general conclusions and points out the need for further study, and in particular the need for an engineering feasibility study. Let us summarize here some specific conclusions reached in the report.

(i) From Fig. 2.2a, we see that at small latitudes $\Lambda \lesssim 40°$ N,S a fully steerable telescope (FST) that can point at the horizon can cover practically the entire sky, whereas an almucantar radio telescope (ART) with Z_{MAX} = 30° and any ΔZ can cover about half that much. Since observations are seldom made near the horizon at least at short centimeter and millimeter wavelengths, the maximum zenith angle of the FST should be more like Z_{MAX} = 60° which is shown in Figure 2.2b. In terms of sky coverage, the FST has an advantage over the ART insofar as it can cover more sky by about a factor 1.75 at low latitudes, independent of the degree ΔZ of steerability in elevation (see also (vi) below)

(ii) Figures 3.3 a-f and 4.1 a-c deal with the lesser important factor τ in the expression (0.1) above. The figures 3.3 a-f given τ in the form of a differential hour angle ΔH during which one source can be observed or tracked, on one or other side of the meridian, as a function of the degree ΔZ of elevation steerability. In practice, a source distribution is what needs to be observed, and figures 4.1 a-c gives $F(\delta)$, the total time in a day (observations on both sides of the meridian) per unit beamwidth (in

time units) for a point source lying along a range in right ascension of 1 hour at the equator (secant δ hours at declination δ, with an appropriate guillotine near the poles). The integration times per unit beamwidth for the ART are seen to have greatly increased compared to those for the FST, because the rotation of the earth assists the ART in sweeping across the source distribution. With $\tau = F(\delta)\beta \sim F(\delta)\lambda/D$, equation (0.1) gives $S_\nu \sim 1/D^{3/2} F^{1/2}(\delta)$, so that the ART with ΔZ small is equally as sensitive as the FST when $D_{ART} \approx 2 D_{FST}$. As the required task is defined to cover larger and larger ranges in right ascension, the advantage of full steerability essentially disappears for source distributions accessible to both telescopes (see also (vi) below on sky coverage)

(iii) To compare capabilities of the ART with those of the FST for the source counting problem, it is necessary to choose some cosmological model. The usual choice is a Euclidean model, with sources of some average constant spectral index. With this choice, Figure 5.4 compares as a function of λ the counts obtained in a year by a gravitational-deflection limited FST according to von Hoerner's expression $D_{FST} = 434\sqrt{\lambda}$ meters with a $D_{ART} = 300$ meters. Particularly at shorter wavelengths, a smaller value of D_{ART} would be more realistic but the principle of this example calculation remains the same, viz., that however large the FST can be built, the ART can be designed to outperform it for the cosmological source counting problem.

(iv) Results for variable quasi-stellar-source monitoring are shown in Figure 5.6 for $\lambda = 3$ cm. The result is intuitively obvious from equation (0.1), that the larger D possible for the ART permits monitoring of much fainter sources than can be monitored with the FST.

(v)   It is well-known that source counting is sensitivity-limited at short wavelengths. Figures 5.3 and 5.4 show that the greatest need is for large collecting areas at short centimeter and millimeter wavelengths. At these wavelengths, structures become highly sensitive to environmental conditions (wind loads, temperature gradients across the structure). The need is therefore for a radome to house say a 100 meter or 125 meter almucantar telescope for operation at millimeter wavelengths, and therefore particularly for an engineering feasibility study of a radome-almucantar telescope combination.

(vi)   Chapter 6 lists the limits on D for fully steerable telescopes, as found by von Hoerner, and concludes that an almucantar telescope that is non-environmental (e.g. radome enclosed) can exceed in size the largest FST by a large factor, though this factor is not yet known. The need for an engineering feasibility study is therefore once more evident. It is pointed out that the ART design uses nature to advantage in achieving small minimum detectable flux densities, even to the point where the earth itself can perform some of the functions of a radome. The Chapter concludes with a rule-of-thumb discussion of cost, pointing out that the cost of FST goes (it is believed) as D^3 for small D but for large D singular factors like $(D_{MAX, \; FST} - D)^{-1}$ arise that make the cost of large FST prohibitive. By contrast, the cost of the ART should go more like D^2 for $D >> D_{MAX, FST}$. Further, the cost argument points the way to achieving sky coverage for ART equal to or greater than FST; complete sky coverage for ART can be obtained by an arithmetic increase in the cost of a basically inexpensive unit (two or three ART at

different geographical latitudes) whereas a single FST at the earth's equator

achieves full sky coverage but is singularly expensive and lacking in comparable

sensitivity and resolution.

1. Introduction

The almucantar radio telescope is defined to be a paraboloidal reflector free to rotate in azimuth (i.e. about an axis perpendicular to the ground) but free to move in altitude (i.e. elevation) only between two angles Z_{MAX} and Z_{MIN} from the zenith, such that sources lying between two small circles parallel with the horizon (almucantars) are accessible at any one instant. Almucantars are parallels of altitude, or small circles parallel to the observer's horizon (Chauvenet 1863).

The concept of almucantar antennas is an outgrowth of a proposal (Usher 1963) to save the 600 foot telescope at Sugar Grove, West Virginia by turning it into a fixed elevation transit instrument. Simply speaking, an almucantar antenna is an intermediate case between the two extremes of fully steerable and transit telescopes. For single paraboloidal dishes, there is of course no substitute for full steerability, but this can be achieved only for relatively smaller dish sizes and relatively longer wavelengths, with a resultant loss in resolution. To increase resolution by decreasing λ for a given D, specifications on surface tolerance of large dishes become tighter, and steerability must be limited. To minimize surface deflections, the limitation in steerability must clearly be in elevation rather than in azimuth, but this will entail a loss in sky coverage. We can therefore say:

I.   To maximize gain at the expense of sky coverage, a paraboloidal antenna should be limited in zenith angle steerability.

but that:

II.   There exists a range in zenith angle (no matter how small) through which the aperture of an antenna can be moved and still maintain a specified surface tolerance.

Statements I and II provide the necessary motivation for a preliminary reconnaissance of the capabilities of the almucantar radio telescope (ART). How such a telescope could be designed is discussed in Chapter 6, to which the reader might like to go first for an overview.

In Chapters 2-4 we work out some of the basic geometrical considerations in the almucantar design. These Chapters could well be skimmed to avoid bogging down, since for the sake of completeness we present results to the complexity that they have been worked out so far. Chapter 5 explores the capabilities of the almucantar telescope for source counting and for monitoring which are essential to a resolution of the cosmological problem. Finally, our conclusions are stated in Chapter 7.

2. Sky Coverage

2.1 Diurnal sky coverage

The solid angle of sky accessible to observation by an almucantar antenna during 24 sidereal hours is given as a function of latitude Λ, by

$$\Omega = 2\pi \left\{ \sin \Theta - \sin (\Lambda - Z_{Max}) \right\} \tag{2.1a}$$

where there are three cases for Θ (see Figure 2.1):

$$
\begin{array}{ll}
1. & \Theta = \Lambda + Z_{MAX} \\
2. & \Theta = \pi/2 \\
3. & \Theta = \Lambda + Z_{MIN}
\end{array}
\right\} \text{ according as }
\left\{
\begin{array}{l}
(\Lambda + Z_{MIN} \leq) \pi/2 \geq \Lambda + Z_{MAX} \\
\Lambda + Z_{MIN} \leq \pi/2 \leq \Lambda + Z_{MAX} \\
\Lambda + Z_{MIN} \geq \pi/2 (\leq \Lambda + Z_{MAX})
\end{array}
\right.
\tag{2.1b}
$$

These respective cases occur when the celestial pole lies (1) outside the Z_{MAX} almucantar, (2) between the Z_{MAX} and Z_{MIN} almucantar, and (3) inside the Z_{MIN} almucantar.

We let

$$Z_{MAX} - Z_{MIN} = \Delta Z \tag{2.2}$$

which is the degree of altitude steerability. Figures 2.2 (a-d) give Ω as a function of Λ, Z_{MAX} and ΔZ, for $Z_{MAX} = 0°$ to $90°$ and $\Delta Z = 0°$ to Z_{MAX} in increments of $10°$. Figure 2.3 is an aid to reading these graphs, which show firstly, Ω and the three domains of Eqns. (2.1 a,b); secondly, the difference $\Delta\Omega_1 = 2\pi \left\{ 1 - \sin (\Lambda + Z_{MAX}) \right\}$, and lastly the difference $\Delta\Omega_3 = 2\pi \left\{ 1 - \sin (\Lambda + Z_{MIN}) \right\}$, where $\Delta\Omega_1$ and $\Delta\Omega_3$ are the circumpolar solid angles of the sky inaccessible to the almucantar antenna in cases 1 and 3 above. The instantaneous sky coverage is depicted in Figure 2.4 on an Aitoff equal area projection of the celestial sphere for the special cases $Z_{MAX} = 30°, 40°,$

$\Lambda = 40°$ and $Z_{MAX} = 30°$, $\Lambda = + 20°$. Also shown in the figure is the Milky Way, the Magellanic Clouds, and the ecliptic.

Special numerical values for Ω in expression (2.1a) are listed in Table 3.2.

2.2 Milky Way Sky Coverage

A sadly neglected area in spherical geometry is that bounded by three or more small circles. It is necessary to evaluate such areas in order to answer practical questions such as - what is the fraction of the Milky Way accessible to observations from a particular locale, such that secant Z values do not exceed a specified amount?

To proceed with this question, we must first find the general equation for a small circle. We rotate axes to bring a right circular cylinder (whose intersection with the sphere is generally a small circle) into an arbitrary orientation shown in Figure 2.5, starting with the cylinder's axis coinciding with the ζ-axis, the first rotation occurs about the ζ-axis through an angle $(90 - \Lambda^*)$, followed by a rotation about the ζ-axis through angle α_o. The small circles are given by the solution of

$$\cos^2 \delta \sin^2 (\alpha - \alpha_o) + \left\{ \sin \Lambda^* \cos \delta \cos (\alpha - \alpha_o) - \cos \Lambda^* \sin \delta \right\}^2 = \sin^2 Z^* \qquad (2.3)$$

where α, δ are the right ascension and declination and Z^* is the angular distance between the axis of the cylinder and any point of intersection of the cylinder with the sphere. From the element of solid angle

$$d^2 \Omega = \cos \delta \, d \delta \, d \alpha$$

the integrated solid angle between (for example) any two small circles and a great circle of constant α is (for small $\Delta \alpha$)

$$\Omega = \Delta \alpha \sum_{i=1}^{n} \int_{\delta_1(\alpha_i)}^{\delta_2(\alpha_i)} \cos \delta \, d \delta = \Delta \alpha \sum_{i=1}^{n} \left\{ \sin \delta_2(\alpha_i) - \sin \delta_1 (\alpha_i) \right\} \qquad (2.4)$$

where δ_1, δ_2 are calculated from Eq. (2.3) (or, at the intersections, simply deduced from the geometry) when i and hence α_i are specified. Adding together the solid angles for any number of such small-circle triangles gives the solid angle of an arbitrary small-circle polygon. (The necessarily hazy definition of the Milky Way does not require more accuration integration formulae than (2.4)).

We approximate the Milky Way by two small circles each at an angular distance of 7° from the galactic equator which we assume is inclined to the celestial equator by 63°. Thus $\Lambda^* = 27°$, $Z^*_{MAX} = 97°$, $Z^*_{MIN} = 83°$, and the total solid angle of the Milky Way is $\Omega_{MW} = 4\pi(0.1219)$ where $\sin 7° = 0.1219$.

The excessive topological complexity of Milky Way solid angles accessible to observers with arbitrary Z_{MAX}, ΔZ and Λ precludes a complete evaluation like that in section 2.1 above. Consequently, we have evaluated Ω_{MW} for $Z_{MAX} = 30°$, 40°, 60° and 90° for all $0° \leq |\Lambda| \leq 90°$ with the results shown in Figure 2.6. In all cases, we assume $\Delta Z = Z_{MAX}$, i.e. a fully steerable telescope within the limits of Z_{MAX}. In practice, this limitation on ΔZ is of no importance, since only for (probably impractical) latitudes greater than 70° N or S is there any relative diminution in Ω_{MW} due to this effect.

The maxima in the curves come about from the fact that, as (say northern) latitudes increase, the loss in Milky Way coverage in the Southern sky is more than offset by the gain in the Northern sky; this gain ceases near the northern limit of the Milky Way, whereupon increasing the latitude simply results in decreasing the Milky Way coverage. Thus, if a telescope is to be built with $Z_{MAX} = 30°$ or 40° say (irrespective of ΔZ), an optimum Milky Way coverage is obtained from middle latitudes near 30° to 40° N and S.

3. ## Properties of the hour angle function ΔH

   3.1 _Derivation and analysis_

   The function $\Delta H\ (\delta;\ \Lambda,\ Z_{MAX},\ Z_{MIN})$ gives the time taken for a source, on

either side of the meridian and at declination δ, to move between the zenith distances

Z_{MAX} and Z_{MIN} when viewed from latitude Λ (see Fig. 3.1) neglecting atmospheric

refraction. The expression for ΔH that is valid between declinations $\Lambda \pm Z_{MIN}$ can be

found from a double application of the cosine formula of the astronomical triangle (e.g.

$NCP/Z/S_1$ in Fig. 3.1 in which H_{MAX} and H_{MIN} are defined). We let

$$\Delta H = H_{MAX} - H_{MIN} \tag{3.1}$$

$$a = \cos H_{MAX} \tag{3.2a}$$

$$b = \cos H_{MIN} \tag{3.2b}$$

and it follows when

$$\Lambda - Z_{MIN} \leq \delta \leq \Lambda + Z_{MIN} \tag{3.3}$$

that

$$\Delta H = \cos^{-1} \left\{ ab + \sqrt{(1 - a^2)(1 - b^2)} \right\} \tag{3.4}$$

where

$$a = \cos Z_{MAX} \sec \delta \sec \Lambda - \tan \delta \tan \Lambda \tag{3.5a}$$

$$b = \cos Z_{MIN} \sec \delta \sec \Lambda - \tan \delta \tan \Lambda \tag{3.5b}$$

When either

$$\Lambda + Z_{MIN} \leq \delta \leq \Lambda + Z_{MAX} \tag{3.6a}$$

or

$$\Lambda - Z_{MAX} \leq \delta \leq \Lambda - Z_{MIN} \tag{3.6b}$$

we have simply the expression for the hour angle east or west of the meridian:

$$H \equiv \Delta H = \cos^{-1} a \tag{3.7}$$

(ΔH may be converted to units of time through $\pi/12$ radians = $15°$ = 1 hour, 15 arc minute = 1 time minute, 15 arc second = 1 time second)

We note the following points:

(1) Expressions (3.4) and (3.7) for ΔH are identical at the interfaces $\delta = \Lambda + Z_{MIN}$ between the domains of Eqs. (3.3) and (3.6); for then $\cos Z_{MIN} = \cos (\Lambda - \delta)$, hence from Eq. (3.5b), b = 1 and then Eq. (3.4) reduces to Eq. (3.7).

(2) It appears that expression (3.4) for $\cos \Delta H$ could be the root of a quadratic and, in fact, can be so derived by (for example) eliminating H_{MAX} from Eq. (3.2a) using Eq. (3.1), then expanding the cosine of the sum of the angles H_{MIN} and ΔH, and subtracting from it $\cos \Delta H$ times Eq. (3.5b). We get

$$\sin H_{MIN} \sin \Delta H = S (\cos Z_{MIN} \cos \Delta H - \cos Z_{MAX}) - T (\cos \Delta H - 1) \tag{3.8}$$

where

$$S \equiv \sec \delta \sec \Lambda \tag{3.9a}$$

$$T \equiv \tan \delta \tan \Lambda \tag{3.9b}$$

Now on multiplying (3.5b) by sin ΔH, squaring and adding to the square of Eq. (3.8),

we have a quadratic in cos ΔH:

$$\cos^2 \Delta H - 2 \cos \Delta H \, (S \cos Z_{MAX} - T)(S \cos Z_{MIN} - T) + U = 0 \qquad (3.10)$$

where

$$U = S^2 (\cos^2 Z_{MIN} + \cos^2 Z_{MAX}) - 2 ST (\cos Z_{MIN} + \cos Z_{MAX}) + 2 T^2 - 1.$$

After some further manipulation, the solution to expression (3.10) reduces to Eq. (3.4).

(3) The expression (3.4) has a minimum when

$$\sin \delta = \sin \Lambda \, \frac{1 + \cos (Z_{MAX} + Z_{MIN})}{\cos Z_{MAX} + \cos Z_{MIN}} \qquad (3.11)$$

as can be ascertained at least by tedious algebra.

3.2 A Special case of fixed elevation

Consider the limit $\Delta Z/2 = \chi \rightarrow 0$ where by Eq. (2.2)

$$Z_{MAX} - Z_{MIN} = 2\chi. \qquad (3.12)$$

Let

$$Z = \tfrac{1}{2}(Z_{MAX} + Z_{MIN}). \qquad (3.13)$$

Hence

$$Z_{MAX} = Z + \chi, \qquad (3.14a)$$

$$Z_{MIN} = Z - \chi. \qquad (3.14b)$$

It follows from Eqns. (3.5) and (3.14) that

$$a = S \cos Z - T + \chi S \sin Z - \tfrac{1}{2} \chi^2 S \cos Z + O(\chi^3),$$

$$b = S \cos Z - T - \chi S \cos Z \div \tfrac{1}{2} \chi^2 S \cos Z + O(\chi^3),$$

whereupon Eq. (3.4) gives

$$\cos \Delta H = 1 + \frac{2 \chi^2 S^2 \sin^2 Z}{(S \cos Z - T)^2 - 1} + O(\chi^4).$$

Hence with the help of definition (3.9)

$$\frac{\Delta H}{2\chi} = \frac{\sin Z \sec \delta \sec \Lambda}{\sqrt{1 - (\cos Z \sec \delta \sec \Lambda - \tan \delta \tan \Lambda)^2}}, \qquad (3.15)$$

for small χ. If we identify 2χ with the half power beam width (HPBW) of a telescope,

expression (3.15) gives the time ΔH taken for a source to pass through the beam

when the source is tracked in azimuth (i.e. the telescope is moved in azimuth to

compensate for the decreasing zenith distance between the time when the source first

"enters" the HPBW at S_1 and when it "leaves" at S_2, see figure 3.2). This time

ΔH is proportional to the HPBW to first order in χ.

We note the following points:

(1) We may regard the difference $Z_{MAX} - Z_{MIN}$ in expression (3.12) as a

differential ΔZ, whereupon the distinction between Z_{MAX} and Z_{MIN} becomes

negligible and each may be replaced by (say) Z. Then Eq. (3.15) becomes an

expression for $\frac{\partial H}{\partial Z}$ whose form can be verified by differentiation of Eq. (3.7).

(2) Setting the partial derivative with respect to δ of (3.15) equal to zero,

we find that ΔH is a minimum in this case when

$$\sin \delta = \cos Z \sin \Lambda. \qquad (3.16)$$

This agrees with (3.11) when $Z_{MAX} = Z_{MIN} = Z + O(\chi)$. Furthermore, in this approximation, the value of ΔH there is just $2 \chi \sec \Lambda$.

(3) The limits (3.3) of applicability in this case are

$$\Lambda - (Z - \chi) \leq \delta \leq \Lambda + (Z - \chi) \tag{3.17}$$

by use of Eq. (3.14b). Since $\chi < < \left| \Lambda \pm Z \right|$, then for all practical purposes

$$\Lambda - Z \leq \delta \leq \Lambda + Z. \tag{3.18}$$

However, near these limits the approximate equation (3.15) breaks down, as can be verified by setting $Z = \pm (\Lambda - \delta)$ and observing the singularity.

(4) Consequently, at the limits (3.17), we use the exact expressions (3.4) and (3.7) to get ΔH. At $\delta = \Lambda + Z - \chi$, it can be shown that $a = 1$ and

$$\Delta H = \cos^{-1} \left[1 - \frac{2 \sin Z \sin \chi}{\cos \Lambda \cos (\Lambda + Z - \chi)} \right] \tag{3.19}$$

and at $\delta = \Lambda - Z + \chi$, $b = 1$ and

$$\Delta H = \cos^{-1} \left[1 - \frac{2 \sin Z \sin \chi}{\cos \Lambda \cos (\Lambda - Z + \chi)} \right] \tag{3.20}$$

(5) Very little interest attaches to the equivalent of equations (3.6) and (3.7) in this last case, because the declination range is 2χ (or one HPBW) and is negligibly small.

(6) When the telescope does not track in azimuth, i.e. it is used as a pure transit instrument,

$$\Delta H = 2\chi \sec \delta. \tag{3.21}$$

In this case, once again there is little interest in the fine details of ΔH near the northern and southern extremities of its almucantar.

3.3 Catalogue of other cases

For reference purposes, we record here the different possibilities (cf Figure 3.1) and the values for the hour angles East or West of the meridian. For convenience, we have assumed $\Lambda \geq 0$.

Case 1 $\Lambda + Z_{MAX} \leq 90°$

$\Lambda + Z_{MAX} \geq \delta \geq \Lambda + Z_{MIN}$ $\cos \Delta H = a$

$\Lambda + Z_{MIN} \geq \delta \geq \Lambda - Z_{MIN}$ $\cos \Delta H = ab + \sqrt{(1 - a^2)(1 - b^2)}$

$\Lambda - Z_{MIN} \geq \delta \geq \Lambda - Z_{MAX}$ $\cos \Delta H = a$

Case 2 $\Lambda + Z_{MIN} > 90°$, $\Lambda + Z_{MIN} \leq 90°$

(i) $\Lambda + Z_{MIN} < 180° - (\Lambda + Z_{MAX})$

$90° \geq \delta \geq 180 - (\Lambda + Z_{MAX})$ $\Delta H = 12^h$

$180 - (\Lambda + Z_{MAX}) \geq \delta \geq \Lambda + Z_{MIN}$ $\cos \Delta H = a$

$\Lambda + Z_{MIN} \geq \delta \geq \Lambda - Z_{MIN}$ $\cos \Delta H = ab + \sqrt{(1 - a^2)(1 - b^2)}$

$\Lambda - Z_{MIN} \geq \delta \geq \Lambda - Z_{MAX}$ $\cos \Delta H = a$

(ii) $\Lambda + Z_{MIN} > 180° - (\Lambda + Z_{MAX})$

$90° \geq \delta \geq \Lambda + Z_{MIN}$ $\Delta H = 12^h$

$\Lambda + Z_{MIN} \geq \delta \geq \Lambda - Z_{MIN}$ $\cos \Delta H = -b$

$\Lambda - Z_{MIN} \geq \delta \geq 180° - (\Lambda + Z_{MAX})$ $\Delta H = 12^h$

$180 - (\Lambda + Z_{MAX}) \geq \delta \geq \Lambda - Z_{MAX}$ $\cos \Delta H = a$

<u>Case 3</u> $\Lambda + Z_{MIN} > 90°$

$$180° - (\Lambda + Z_{MIN}) \geq \delta \geq 180° - (\Lambda + Z_{MAX}) \qquad \cos \Delta H = -b$$

$$180° - (\Lambda + Z_{MAX}) \geq \delta \geq \Lambda - Z_{MIN} \qquad \cos \Delta H = ab + \sqrt{(1 - a^2)(1 - b^2)}$$

$$\Lambda - Z_{MIN} \geq \delta \geq \Lambda - Z_{MAX} \qquad \cos \Delta H = a$$

At some limits ΔH appears to be discontinuous. This is due to the assumption that the beamwidth is vanishingly small.

Table 3.1

Average time <ΔH> that a point source is accessible to an antenna with given Λ, Z_{MAX} and ΔZ characteristics, when pointed either east, or west of the meridian. The total average times per day are 2<ΔH> . Times are in seconds, angles in degrees. (cf Figures 3.3(a-f)) Digits in parentheses denote powers of ten.

Z_{MAX} ⟍Λ ΔZ	0	±20	±40
30 0(*)	4.196(0)	4.530(0)	5.959(0)
30 1	3.796(2)	4.082(2)	5.266(2)
30 2	7.456(2)	8.015(2)	1.032(3)
30 5	1.764(3)	1.894(3)	2.424(3)
30 10	3.197(3)	3.427(3)	4.355(3)
30 30	5.722(3)	6.121(3)	7.690(3)
40 0(*)	4.371(0)	4.794(0)	6.979(0)
40 1	3.894(2)	4.236(2)	5.881(2)
40 2	7.679(2)	8.347(2)	1.153(3)
40 5	1.840(3)	1.996(3)	2.717(3)
40 10	3.417(3)	3.696(3)	4.947(3)
40 20	5.814(3)	6.267(3)	8.213(3)
40 40	7.708(3)	8.287(3)	1.071(4)
60 60	1.197(4)	1.320(4)	2.023(4)
90 90	2.160(4)	2.428(4)	2.774(4)

(*) entries for these cases are Times (seconds) per HPBW (arc minutes) for no azimuthal tracking; see equation (3.15).

Table 3.2

Fractional Sky Coverage for telescope of given Λ, Z_{MAX} and ΔZ characteristics, evaluated from equation (2.1).

Z_{MAX}	ΔZ $\diagdown$ Λ	0	± 20	± 40
30	0 to 30	0.50	0.47	0.38
40	0 to 40	0.64	0.61	0.49
60	60	0.86	0.82	0.67
90	90	1.00	0.97	0.88

3.4 Graphical results for ΔH at particular latitudes

The values of ΔH derived above are presented in graphical form in Figures 3.3(a-f) for those values of Λ, Z_{MAX} and ΔZ listed in Table (3.1). The entries in Table (3.1) are average times that a point source is accessible to observation on one side of the meridian or the other. Total times per day are double the values given in the Figures and the Tables. In addition, Table (3.2) gives the fractional sky coverage for these cases as deduced from Section (2.1).

Figures 3.3(a-f) also contain the following information: the dot-dash curves intersect each ΔZ curve at its minimum as predicted by expression (3.11); they do not extend quite to the cases $Z_{MIN} = 0$ (i.e. $\Delta Z = Z_{MAX}$) for which there are, strictly speaking, no minima, even though Eq. (3.11) predicts the correct limiting values of $\delta = \Lambda$ in these cases. Physical significance is attached, however, to the cases $\Delta Z = 0$ (i.e. $Z_{MIN} = Z_{MAX}$) for which expression (3.11) predicts $\sin \delta = \sin \Lambda \cos Z_{MAX}$. These latter cases relate to the curves marked $\Delta Z = 0$ (AT) for which a telescope of fixed tilt tracks a source in azimuth in accordance with the special case of section 3.2. Here ΔH is proportional to 2χ (= HPBW) by expression (3.15); hence, we have presented the $\Delta Z = 0$ curves in Figures 3.3(a-f) with the choice of HPBW = 1 arc minute. It is therefore a simple matter to deduce other curves for the $\Delta Z = 0$ cases by multiplying the ΔH values by the required HPBW in arc minutes (i.e. by adding or subtracting the log of the HPBW in arc minutes over most of the range in δ for which the linear $\Delta H \propto \chi$ relation (3.15) holds.) The HPBW is further related to the diameter D and operating wavelength λ (in the same units) by the theoretical relation β (the HPBW in radians) $= \dfrac{4\lambda}{\pi D}$ which is given in nomogram form in Fig. 3.4. This nomogram thus further facilitates a rapid exploration of different possibilities for the $\Delta Z = 0$ (and other) cases. The

branches of the $\Delta Z = 0$ curves labeled (NAT) refer to the values for no azimuthal tracking (Eq. 3.21). Finally, if it is of interest to locate the precise maximum at the southern and northern limits of the $\Delta Z = 0$ (AT) curves, these can be found from expressions (3.19) and (3.20); more detailed analysis of the Figures to terms of order χ does not seem profitable at present.

3.5 Discussion

Two major conclusions are evident from Figures 3.3 (a-f). The first is that as the HPBW β becomes smaller and smaller (antenna aperture larger and larger for a given wavelength) the time available to a fixed elevation telescope for a point source becomes smaller and smaller, whereas if the telescope is designed with elevation steerability that is even as small as 1°, about 300 seconds of continuous integration time on a source are available in half a day independent of aperture. For example, for a dish with $\beta = 1$ arc minute (400 ft. aperture at 3 cm) with $\Delta Z = 1°$ compared to $\Delta Z = 0$, we see that ΔH is larger by a factor of about 10^2, which translates into a decrease in the minimum detectable flux by a factor of 10 (see Eq. 5.3).

The second conclusion is that a further increase by a factor of 10^2 in the ΔH integration time can only be achieved by increasing ΔZ from 1° to about 60°, which for large dishes is mechanically difficult if indeed it can be achieved at all. In fact, it is approximately correct to say for a 600 ft. dish at 3 cm that

$$100 \approx \frac{\Delta H (\Delta Z = Z_{MAX} = 90°)}{\Delta H (\Delta Z = 1°, \ Z_{MAX} \sim 30°)} \approx \frac{\Delta H (\Delta Z = 1°, \ Z_{MAX} \sim 30)}{\Delta H (\Delta Z = 0, \ Z_{MAX} \sim 30)}$$

which clearly spells out the advantage of striving for azimuth steerable telescopes with even a modicum $\Delta Z \sim 1°$ of steerability in altitude. How this can be achieved is discussed in Chapter 6.

A minor conclusion that is apparent from Figures 3.3 (a-f) is that ΔH for a transit telescope fixed in elevation and tracking in azimuth (the curves labeled AT) is larger on the average than ΔH for a transit telescope fixed in azimuth which is incapable of azimuthal tracking (the curves labeled NAT).

All three conclusions provide justification for exploring the consequences of Statements I and II of Chapter 1.

4. Properties of the hour angle function for extended source distributions

4.1 Preliminary remarks

We have shown in Chapter 3 that ΔH is the time that a point source is accessible to the almucantar antenna on either side of the meridian. But in an extended region of sky with a range $\Delta \alpha$ in right ascension, the time during which sources in this range can be observed is $\Delta H + \Delta \alpha$. This follows from the fact (cf Figure 3.1) that on the eastern side of the meridian the most westerly (preceding) point of the region is accessible to the telescope first at maximum zenith angle and as the earth turns the most easterly (following) point is accessible last at the minimum zenith angle. (On the western side of the meridian, the process is reversed since the preceding or westerly point is first detected at minimum zenith angle.) In the limit $\Delta H \rightarrow 0$ (i.e. $\Delta Z \rightarrow 0$) the time is just $\Delta \alpha$, the time taken for a stationary beam to sweep across the source distribution. It follows that as the capabilities of the antenna are made more flexible by allowing a finite elevation steerability, $\Delta \alpha$ is increased by the amount of time ΔH that the source distribution can be followed.

Conversely, once the goal to map a region of the sky is decided upon, the total time spent integrating on the distribution of sources can be quite substantially increased over ΔH, at the expense, of course, of the time on any one point in the distribution. This corroborates the view that almucantar antennas are especially suited for sky surveys, while at the same time retaining the flexibility of some degree of elevation steerability for the study of individual point sources.

4.2 Solid angle of extended distributions

Consider a source distribution bounded by declination δ_1 and δ_2 and right ascension α_1 and α_2, where

$$\delta_2 + \delta_1 = 2\delta, \tag{4.1a}$$

$$\delta_2 - \delta_1 = \Delta\delta, \tag{4.1b}$$

$$\alpha_2 - \alpha_1 = \Delta\alpha. \tag{4.1c}$$

The solid angle of sky contained within these boundaries is

$$\Omega = \Delta\alpha \cos\delta \, (2 \sin\tfrac{1}{2}\Delta\delta). \tag{4.2a}$$

When the declination range $\Delta\delta$ is small,

$$\Omega = \Delta\alpha \cos\delta \, (\Delta\delta + \text{terms in } \Delta\delta^3) \tag{4.2b}$$

In either case (4.2a or b), when mapping occurs over a given solid angle and declination range, we require $\Delta\alpha \cos\delta = \text{constant}$, or $\Delta\alpha = \text{constant}/\cos\delta$. We define $\Delta\alpha_{eq}$ to be the range of right ascension at the equator, that will produce a given Ω for a specified $\Delta\delta$ range about δ, i.e.

$$\Delta\alpha(\delta) = \text{smaller of } \begin{cases} \Delta\alpha_{eq}/\cos\delta \\ 24^h \end{cases} \tag{4.3}$$

(For example, suppose we wish to count sources over a portion of sky that is "square"; then if the range of right ascension of that region is $\Delta\alpha_{eq}$ at the equator, it is $\Delta\alpha_{eq}/\cos\delta$ at declination δ, and in any event is never greater than 24 hours; thus if $\Delta\alpha = 1^h$, then $\Delta\alpha = 24^h$ for $|\delta| \geq \cos^{-1}(1/24)$ or $87°37'$.)

4.3 Integration times

Consider a HPBW of β. At the equator this has a certain equivalent in time units which we call $\beta_{t,eq}$. The range in right ascension covered by β at declination δ is thus $\beta_{t,eq}/\cos\delta$ (which, of course, must not exceed 24^h). For simplicity we

suppose that the integration time on a point source is the time that the source spends within the HPBW. At a particular δ, these sources are spread out over a range in right ascension of $\Delta \alpha$, and the time spent integrating on these sources is $\Delta \alpha(\delta) + \Delta H(\delta)$. Therefore, if a time $\Delta \alpha(\delta) + \Delta H(\delta)$ is spent covering sources along a range $\Delta \alpha(\delta)$, then the time τ^* spent on <u>either</u> side of the meridian covering one HPBW at δ is

$$\tau^* = \frac{\beta_{t,eq}}{\cos \delta} \frac{\Delta \alpha(\delta) + \Delta H(\delta)}{\Delta \alpha(\delta)} \qquad (4.4)$$

which, in the absence of source confusion (cf Section 5.1) is the integration time for a point source during one scan of the raster.

Equation (4.4) has the following limits:

(1) When $\Delta H = 0$, i.e. for $\Delta Z = 0$, equation (4.4) reduces to (3.21) vis., $\tau^* = \beta_{t,eq} \sec \delta$, which gives the integration time for a single transit of a point source.

(2) When $\Delta H \neq 0$ and this time is spent tracking on one source, then $\Delta \alpha \rightarrow \frac{\beta_{t,eq}}{\cos \delta} < < \Delta H$ and Equation (4.4) reduces simply to

$$\tau^* = \Delta H(\delta)$$

which are the times given in Figures 3.3(a-f) for tracking on one source.

Expression (4.4) gives the integration time on a point source along a right ascension range of $\Delta \alpha$ at declination δ during a scan over an hour angle of $\Delta H(\delta)$ on one side of the meridian. However, almucantar antennas have the feature that sources are accessible on both sides of the meridian. We have the following cases (cf Figure 3.1):

(i) $\Lambda + Z_{MIN} \leq \delta \leq \Lambda + Z_{MAX}$ and $\Lambda - Z_{MAX} \leq \delta \leq \Lambda - Z_{MIN}$.

These regions correspond to Equation (3.6 a,b) for which $\Delta H(\delta)$ is given by Equation (3.7), and is thus measured from the meridian. Here one half the $\Delta \alpha$ range is tracked on the eastern side of the meridian over $\left| \Delta H \right|$, the other half on the western side also over $\left| \Delta H \right|$. Consequently, the integration time for some point in a day is

$$\tau^* = \frac{\beta_{t,eq}}{\cos \delta} \frac{\frac{1}{2} \Delta \alpha + \Delta H}{\frac{1}{2} \Delta \alpha} \quad \text{or}$$

$$\tau^* = \frac{\beta_{t,eq}}{\cos \delta} \frac{\Delta \alpha (\delta) + 2 \Delta H(\delta)}{\Delta \alpha (\delta)} \tag{4.5}$$

(ii) $\Lambda - Z_{MIN} \leq \delta \leq \Lambda + Z_{MIN}$.

Two sub-cases are apparent depending on whether there exists or does not exist a range of δ between these limits for which

$$\Delta \alpha (\delta) \leq 2 \left| H_{MIN} (\delta) \right| \tag{4.6}$$

where $H_{MIN} (\delta) = \cos^{-1} b$ is given by Equations (3.2b) and (3.5b). In other words, if (4.6) holds, then the entire range $\Delta \alpha$ can be observed over ΔH on the eastern side of the meridian, without some portion of the preceding (western) edge of $\Delta \alpha$ becoming accessible on the western side of the meridian. The telescope can then be re-oriented on the western side of the meridian in time to repeat the second scan of $\Delta \alpha$.

But if (4.6) does not hold (as must be the case at least for some declination range near either limit of this case and possibly, if $\Delta \alpha$ is large enough, for the entire declination range) then some other scheme of faster tracking must be devised to maximize the value of τ^*. For this subcase we shall assume for present purposes that Case (i) (eqn. 4.5) holds, i.e. that $1/2 \Delta \alpha$ is tracked on each side of the meridian.

Returning to the subcase for which Equation (4.6) holds, we have for the integration time per day

$$\tau^* = \frac{\beta_{t,eq}}{\cos \delta} \, 2 \, \frac{\Delta\alpha(\delta) + \Delta H(\delta)}{\Delta\alpha(\delta)} \tag{4.7}$$

Combining the cases we have in general

$$\tau^* = \frac{\beta_{t,eq}}{\cos \delta} \, \frac{C_{EW} \, \Delta\alpha(\delta) + 2\,\Delta H(\delta)}{\Delta\alpha(\delta)}$$

where $C_{EW} = 1$ for case (i) and when condition (4.6) does not hold, and $C_{EW} = 2$ when (4.6) does hold, i.e. $C_{EW} = 2$ when two scans per day are possible, otherwise we simply take $C_{EW} = 1$.

For convenience we define

$$F(\delta) = \tau^*/\beta_{t,eq} \tag{4.8}$$

where

$$F(\delta) = \frac{1}{\cos \delta} \left[C_{EW} + \frac{2\,\Delta H(\delta)}{\Delta\alpha(\delta)} \right] \tag{4.9}$$

is the integration time per day, per unit beamwidth, per unconfused point source in the range $\Delta\alpha$. We return to a discussion of $F(\delta)$ in the next section.

The formula (4.9) can also be understood by considering its two parts: firstly, the part $C_{EW}/\cos \delta$ arises from a single transit of a source through the stationary beam (if the source is observed twice in a day, $C_{EW} = 2$; if once, $C_{EW} = 1$), and secondly, the part $\frac{1}{\cos \delta} \, \frac{2\,\Delta H(\delta)}{\Delta\alpha(\delta)}$ is twice the additional integration time gotten on either side of the meridian by moving the telescope through ΔH relative to the sky as sources along $\Delta\alpha$ are scanned. This second part can be simplified by virtue of Equation (4.3) and the discussion preceding it, when a constant scanned area must be maintained; for then $\Delta\alpha(\delta) \cos \delta$ equals the constant $\Delta\alpha_{eq}$, and we have

for the last part $2 \Delta H(\delta)/\Delta \alpha_{eq}$.

Equation (4.9) once again shows the desirability of even a modicum of elevation flexibility in the design of large radio telescopes. Consider for example the mapping of a single source of small angular extent, for which $\Delta \alpha << \Delta H$. Then the last term in Equation (4.9) dominates, and $F(\delta)$ can be substantially increased over the value $C_{EW}/\cos \delta$ that it would have if its elevation were fixed. At the other extreme of mapping the entire sky, this last term in Equation (4.9) vanishes because we must set $\Delta H = 0$ (there is no advantage in tracking because what could be gained in τ^* in one day would be lost the next); thus almucantar telescopes are at no disadvantage, when it comes to mapping the entire sky, and will provide pencil beam resolution that would be otherwise unattainable by a filled aperture telescope.

4.4 Some graphical results for particular cases

The function $F(\delta)$ of Equation (4.9) is shown in Figures 4.1(a-c) for latitudes $\Lambda = 0, \pm 20°, \pm 40°$ and $\Delta \alpha_{eq} = 1$ hour, and various Z_{MAX} and Z_{MIN} ranging from fully steerable to fixed elevation telescopes. The graphs give the integration times per day per half-power beamwidth for a point in a range of right ascension $\Delta \alpha(\delta) = \Delta \alpha_{eq} \sec \delta$. (With $\Delta \alpha_{eq} = 1$ hour, the solid angle for a "square" area of the sky, i.e. $\Delta \delta = 15°$, is $4\pi (0.00544)$ or 0.54% of the celestial sphere; see Section 4.2)

In analysing the function $F(\delta)$ and understanding the Figures 4.1 (a - c), let us first deal with the apparently troublesome singularity at the poles of Equation (4.9). $F(\delta)$ can be re-written

$$F(\delta) = \frac{2}{\Delta \alpha_{eq}} \left[\Delta H(\delta) + \frac{C_{EW} \, \Delta \alpha(\delta)}{2} \right]$$

by virtue of (4.3), and the singularity seems to have disappeared. Actually it lurks

still in $\Delta\alpha(\delta)$ which must be made extremely large if it is to encompass the same

number of sources as $\Delta\alpha(\delta = 0) = \Delta\alpha_{eq}$. But in fact, $\Delta\alpha$ cannot be greater than 24^h;

or, to put it another way, in order to maintain the constant solid angle of sky

$\Omega = \Delta\alpha \cos \delta(2 \sin \frac{1}{2} \Delta\delta)$ as $|\delta|$ increases, then $|\delta|$ must effectively reach a maximum

$|\delta|_{MAX} < 90°$. Nevertheless, the mathematical singularity is not totally devoid of

meaning, because it is certainly possible, for example, to let the beam point at the

very poles for a full 24^h per day, thereby obtaining a good deal more than $24\beta_{t,eq}$

seconds worth of integrating time. But we are ultimately concerned with the reality

of the average behavior over all accessible declinations for a given solid angle of sky,

so we avoid bias in favor of telescopes that are singular in their ability to reach the

poles, by a cut-off in τ^* at 24^h. The resulting average values of $F(\delta)$ given in

Table 4.1 are thereby more realistic in connoting relative capabilities over the ranges

of accessibility.

The fine structure of Figures 4.1(a - c) is probably unwarranted in an

exploratory report of this nature, but serves at least to illustrate graphically the

discussion of cases (i) and (ii), Equations (4.5) - (4.9). For example, $F(\delta)$ when

$\Delta Z = 0°$, $\Delta H = 0$, is just $2/\cos \delta$ and appears in all three figures 4.1(a - c). This

dependence ceases when the condition (4.6) is violated and reverts to $1/\cos \delta$

near the limits $\Lambda \pm Z_{MAX}$ as can be seen in the Figures. A similar argument applies

to cases with $\Delta Z > 0°$ except here, of course, there is a further change in $F(\delta)$ near

the outer limits as $\Delta H(\delta)$ itself changes at $\Lambda \pm Z_{MIN}$; in fact, the behavior of $F(\delta)$

mimics that of $\Delta H(\delta)$ in Figures 3.3 (a - f), but modified by the effect of $\Delta\alpha(\delta)$

and C_{EW}. Approximate values of δ, (correct to $0°5$) for which condition (4.6) is

violated are given in Table 4.2. The full solution for the fine behavior of $F(\delta)$ depends

on the slew rate in azimuth and hence on the telescope characteristics that we are

investigating. (Another interesting problem for the dedicated spherical geometer is to find an expression for the minimum of $F(\delta)$ as a function of $\Delta\alpha_{eq}$.)

The results of Table 4.1 show that there is at most only a factor of about 7 difference in the integration times for a given HPBW between fully steerable and fixed elevation telescopes for $\Delta\alpha_{eq} = 1^h$. Since the horizon to horizon coverage is rarely used in practice, perhaps a factor of 4 would be more realistic. Since the minimum detectable flux S_{ν} goes as $1/D^2\sqrt{\tau}$, a factor of 4 in τ is offset by an increase in D by a factor of $4^{\frac{1}{4}} \sim 1.4$. Again, this is a factor that the almucantar design is easily capable of achieving and exceeding.

Table 4.1

Average values of $F(\delta)$, (the integration time per point source per day per half-power beamwidth in time units) for given almucantar telescope characteristics and latitudes in degrees and $\Delta\alpha_{eq} = 1^h$. Values of the integration time for a point source which lies in a declination range distribution are found by dividing by the number of scans necessary to cover that range in declination.

Z_{MAX} ΔZ Λ		0	± 20	± 40
30	0	2.06	2.21	2.87
30	1	2.23	2.40	3.10
30	2	2.40	2.57	3.32
30	5	2.84	3.06	3.93
30	10	3.45	3.70	4.74
30	30	4.23	4.53	5.76
60	60	7.91	8.86	12.68
90	90	14.66	14.73	16.26

Table 4.2

Values of δ correct to $0°.25$ for which condition (4.6) is violated, for $Z_{MAX} = 30°$. All values are in degrees.

Λ	ΔZ	δ_1	δ_2
0	1	± 27.75	
	2	± 27.00	
	5	± 23.50	
	10	± 18.25	
± 20	1	± 8.25	± 47.75
	2	± 6.75	± 46.75
	5	± 4.00	± 43.25
	10	± 1.25	± 38.00
± 40	1	± 12.00	± 66.75
	2	± 12.75	± 66.00
	5	± 15.75	± 63.00
	10	± 21.00	± 58.00

4.5 Survey times

We wish to distinguish between the times taken to accomplish certain goals by single dishes of various capabilities. Typical projects are (1) mapping of individual sources, (2) mapping the entire accessible sky and (3) mapping of solid angles of the sky for the cosmological problem. Evidently a thorough study is so excessively multi-parametric that some simplifications have to be made. Let us begin by considering only sources near the celestial equator and observers at the geographical equator, and consider almucantar telescopes of $Z_{MAX} = 30°$ and $\Delta Z = 1°$. This greatly simplifies the analysis without much loss of generality. Project (1) covers cases for which almucantar telescopes are least competitive with fully steerable telescopes of a given dish size, while for project (2), they are about equally capable. Project (3) Section 4.5.3 is an intermediate case whose results are used in Chapter 5.

In the following Sections 4.5.1 to 4.5.3 we evaluate the τ/T relation (equations 4.15, 4.18 and 4.24) for the above cases, for fully steerable and almucantar telescopes. (τ in the integration time per source, T the number of days)

4.5.1 Single sources

For single sources we must choose between the analysis of the case of one point source or several. Mutatis mutandis, the most disadvantageous case for almucantar telescopes is that of one point source, so we choose that one.

Suppose that the source is not confused when it lies in a solid angle of C_C half power beam areas (cf Section 5.1), where C_C is of order 50. Suppose further that the area is scanned at successive declinations with separations of C_B HPBW's where C_B is of order 0.5. The square area about the source is $\omega = C_C \pi \beta^2/4$ where we take $\beta = 4\lambda/\pi D$, i.e.

$$\omega = \frac{4 C_C}{\pi} \left(\frac{\lambda}{D} \right)^2 . \tag{4.10}$$

The range in right ascension and declination is (in radians)

$$\Delta\alpha = \Delta\delta = \sqrt{\frac{C_C}{\pi}} \ \frac{2\lambda}{D} . \tag{4.11}$$

The number of scans per raster

$$S = 1 + \frac{\Delta\delta}{C_B \beta} \tag{4.12a}$$

which is thus $1 + \dfrac{\sqrt{\pi C_C}}{2 C_B}$. For $C_C = 50$, $C_B = 0.5$, we see that $\dfrac{\sqrt{\pi C_C}}{2 C_B} = 12.5 >> 1$.

Thus

$$S \approx \frac{\sqrt{\pi C_C}}{2 C_B} \tag{4.12b}$$

We wish to compare capabilities under the following conditions:

(1)   Almucantar telescope, $\Delta H(\delta = 0, \ \Delta Z = 1°)$

(2)   Fully steerable telescope $\Delta H(\delta = 0, \ \Delta Z = 90°)$

each for

(a)   one scan of the raster per day

(b)   one complete raster coverage per day.

Case (a)

For case (a) we have from Equation (4.9) that an integration time of

$\tau^* = \beta_{t,eq} (C_{EW} + \frac{2\Delta H}{\Delta\alpha})$ time units/raster is obtained in S days per raster where

$C_{EW} = 2$ in case (1) and $C_{EW} = 1$ in case (2). Therefore in T sidereal days a point

is integrated upon for a time

$$\tau = \beta_{t,eq} \left[C_{EW} + \frac{2\Delta H}{\Delta \alpha} \right] \frac{T}{S} , \tag{4.13}$$

where

$$T = nS, \ (n \geq 1), \tag{4.14}$$

is the number of days to complete the n rasters of S scans per raster at a rate of 1 scan per day. Equation (4.13) can be rewritten using Equations (4.11) and (4.12):

$$\tau = T \frac{8C_B}{\pi C_C} \left(\Delta H + C_T C_{EW} \sqrt{\frac{C_C}{\pi}} \frac{\lambda}{D} \right) \tag{4.15}$$

where $C_T = 1.375 \times 10^4$ time seconds/radian and λ and D are in meters, T in days, ΔH, and τ in time seconds.

Case (b)

When the task is to be completed in one day, the effective range of right ascension to be covered is $S\Delta\alpha$, and the time available to do it in that day is $C_{EW} \Delta\alpha + 2 \Delta H$. Therefore, the time spent within a HPBW of $\beta_{t,eq}$ is

$$\tau = \frac{\beta_{t,eq}}{S} \left(C_{EW} + \frac{2\Delta H}{\Delta \alpha} \right)$$

which is the same as Equation (4.13) when $T = 1$. Thus Equation (4.13) is a general one for all cases and T may be regarded essentially as a continuous variable with the following provisos: (i) when T is large but not an integer, special tracking requirements are needed to complete the task in a non-integral number of days and (ii) when T is small say $0 \approx 1$ day, special tracking requirements are also needed which will in general depend on source declination. This is true particularly for the almucantar case (1b), in order to utilize all available time in a day. These requirements are also dependent on telescope design which cannot be analysed at this point, but Equation (4.13) will, nevertheless, provide an accurate approximate value in these cases.

4.5.2 Accessible Sky Coverage

Mapping the sky with telescopes of various capabilities raises complex questions on the optimum design of observing programs. Any built-in degrees of freedom in the telescope can be used to decrease the total time for sky coverage , but at the expense of the minimum detectable signal. We avoid these issues by confining our attention to telescopes used as transit instruments, in order to detect the faintest possible sources. In particular we consider a fully steerable telescope and an almucantar telescope with $Z_{MAX} = 30°$.

The following estimates are sufficient for our purposes. The number of drift scans in $\Delta\delta$ separated by C_B parts of a HPBW are $\Delta\delta/C_B\beta$. For

$$\Delta\delta = \pi C_\Delta \qquad (4.16a)$$

say, we have

$$T = \frac{C_\Delta \pi^2}{4 C_B} \frac{D}{\lambda} \text{ days} \qquad (4.16b)$$

where $C_B \sim 0.5$. When $C_\Delta = 1$, this gives an upper limit which for $D = 300$ m, $\lambda = 0.1$ m say is about 1.5×10^4 sidereal days or about 40 years. T is in fact less by a factor of about $C_\Delta = 2/3$ for fully steerable telescopes used at zenith angles less than $60°$, and less by about a factor of $C_\Delta = 1/3$ for almucantar telescopes of $Z_{MAX} = 30°$. The important points to note here are (i) that the almucantar telescope can be duplicated at other locations, so that in fact the sky coverage afforded by one fully steerable telescope can be accomplished simultaneously by two or more

almucantar telescopes, and probably at lower cost (see Chapter 6); and (ii) that a fully steerable paraboloid with $D = 300$ m and $\lambda = 0.1$ m is most likely unrealizable on earth.

We estimate the average integration time on an unconfused source as

$$\tau \approx \beta_t \langle \sec \delta \rangle$$

where the average of sec δ is always finite in reality.

Table 4.3

Average values of sec δ over declination range $\Delta\delta$ for given telescope characteristics.

Λ	Z_{MAX}	$\Delta\delta$		$\langle \sec \delta \rangle$
0	30	-30	+ 30	1.05
	40	-40	+ 40	1.09
± 20	30	-10	+ 50	1.13
	40	-20	+ 60	1.20
± 40	30	+10	+ 70	1.49
	40	0	+ 80	1.75

Table 4.3 gives $\langle \sec \delta \rangle$ for a number of cases, for which we can simply take

$$\tau \approx \beta_t \tag{4.17a}$$

to within a factor of 2. (Comparative evaluations are even less important by factors of $2^{\frac{1}{4}} \approx 1.2$; see discussion following Equation (5.4) below). Thus

$$\tau \approx C_T \frac{4\lambda}{\pi D} \tag{4.17b}$$

time seconds for sky surveys with fully or partially steerable telescopes, where $C_T = 1.375 \times 10^4$ is the number of time seconds per radian. For a given sky area about equal to that for an almucantar telescope ($C_\Delta \approx 1/3$) we have for the unconfused point source integration time

$$\tau \approx T \, \frac{24C_T}{\pi^3} \, (\frac{\lambda}{D})^2 \text{ seconds,} \qquad (4.18)$$

where from Equation (4.16b)

$$T \gtrsim \frac{\pi^2}{6} (\frac{D}{\lambda}) \text{ days,}$$

for one or more complete sky rasters over a declination range given by equation (4.16a) with $C_\Delta = 1/3$. Needless to say, these project times T can become extremely large for high gain antennas. For example, with $D = 300$ m at $\lambda = 3$ cm, T is greater than 4.5 centuries! Clearly, a multiple off-axis system of receivers is called for to reduce these times to reasonable amounts. This calls for a longer focal length Cassegrain design (Christiansen and Högbom 1969) whose properties are ideally suited to the almucantar concept (see Chap. 6).

4.5.3 Partial Sky Coverage

We derive here the τ/T relation for an almucantar telescope that is used primarily as a transit instrument. This will provide a lower limit on its capability as a source-counting machine in the preliminary stages of full sky coverage. In other words, its ability to track in elevation will be ignored, but if it is used, it would provide longer integration times and hence lower minimum flux densities of the observed sources. Thereafter we derive the τ/T relation for a fully steerable

telescope for the same total observing time and equivalent sky coverage, and compare the two capabilities in Chapter 5. In both cases, a total of $1 + \Delta\delta/C_B\beta$ scans, or

$$S \approx \Delta\delta/C_B\beta \qquad (4.19)$$

are required for one raster coverage of a declination range $\Delta\delta$, where successive scans are separated by $C_B\beta$, and occur twice in 24 hours.

Since the almucantar antenna is restricted to its minimum capability as an azimuth steerable fixed elevation transit instrument, the right ascension coverage is 12^h per day (actually slightly less because of the finite slew rate in azimuth) and the integration time on a point source for $C_B \sim 0.5$ is

$$\tau \approx \beta_{t, eq}$$

since for simplicity we are confining our attention to sources near the equator. In T days the integration time is

$$\tau \approx \frac{T}{\frac{1}{2}S} \beta_{t, eq} \qquad (4.20)$$

where the minimum value of T must be $\frac{1}{2}S$ in order to complete one raster. (The factor 2 in Equation (4.20) arises from the fact that one scan over $\Delta\alpha \sim 2 Z_{MAX}$ is made in the eastern hemisphere, followed by the next scan of the chosen area in the western hemisphere, and so on in a day, thus covering slightly less than 12 hours of right ascension). Thus

$$T \geq \tfrac{1}{2}S, \qquad (4.21a)$$

or by Equation (4.19)

$$\Delta\delta \leq 2 C_B T\beta. \qquad (4.21b)$$

On the other hand $\Delta\delta$ must be greater than or about equal to the number of times C_α that the diameter $\sqrt{C_C}\,\beta$ of the confusion circle about a source is exceeded (confusion of sources is discussed in Section 5.1) i.e.

$$\Delta\delta \geq C_\alpha \sqrt{C_C}\,\beta. \tag{4.21c}$$

Combining Equations (4.21b and c), and letting $\beta = 4\lambda/\pi D$, we have

$$\frac{8\,C_B\,T}{\pi}\,\frac{\lambda}{D} \geq \Delta\delta \geq \frac{4\,C_\alpha\sqrt{C_C}}{\pi}\,\frac{\lambda}{D} \tag{4.22}$$

where $\Delta\delta$ is in radians, λ and D in meters, T in days, $C_B \approx 0.5$, $C_C = 50$ and C_α should preferably be at least about 10. To fix ideas, we consider an almucantar antenna with the following characteristics: for example

$$D = 300 \text{ meters}, \quad Z_{MAX} = 30°, \quad \Lambda = 0°, \quad \delta = 0 \pm \Delta\delta; \tag{4.23a}$$

also we choose an area that can be mapped in

$$T = 366 \text{ days with } C_C = 50, \quad C_B = 0.5, \quad C_\alpha = 51.8 \tag{4.23b}$$

for which the equality signs in Equation (4.22) are satisfied, i.e.,

$$T = C_\alpha\sqrt{C_C}/2\,C_B \tag{4.23c}$$

Then we have already

$$\Delta\alpha \approx \pi \text{ radians} \tag{4.23d}$$

and also

$$\Delta\delta \approx 1.55\,\lambda \text{ radians} \tag{4.23e}$$

which varies between $26°6$ at $\lambda = 30$ cm, to $0°89$ at 1 cm; thus these ranges are well within the range of accessibility of the almucantar antenna. Equations (4.19), (4.20), and (4.23e), give the required τ/T relation provided $T \geq 366$ days (Equation 4.21a) and D = 300 meters, i.e.

$$\tau = T \, 1.44 \times 10^3 \, \lambda/D^2 \tag{4.24}$$

We next derive the τ/T relation for a fully steerable telescope, which we assume is being employed on the source-counting job full time, like the almucantar telescope. The area of sky covered with this instrument can be made square, and in fact there must be two squares in opposite hemispheres if the telescope works on one area for 12^h (or 3 squares if it works for 8^h per square, etc.)

In order to compare satisfactorily the capabilities of the two antennas, we must assign them equal areas of the sky and hence equal numbers of potential sources. The area to be surveyed by the fully steerable telescope must be $(\Delta \alpha \Delta \delta)$ to within about 5% or less. Therefore we take the total area to be

$$\Omega = 4.87 \, \lambda \text{ steradians} \tag{4.25}$$

by Equations (4.23d and e). In so doing, we are assigning the sky area to a _fully steerable_ telescope on the basis of an area devised for a 300 meter _almucantar_ telescope. The fact that a _fully steerable_ 300 meter dish (most likely) cannot exist on earth for most λ we are considering, constitutes, of course, one of the main arguments of this report.

Unlike the almucantar antenna, the fully steerable telescope could supposedly cover this entire area in a day or less, but then the number of sources counted will not be significant. Since we have taken 366 days as a reasonable time for such research, it seems most reasonable to compare capabilities over such a time scale or longer.

There is no gainsaying that the shorter the time scale, the more heavily favored is the fully steerable telescope, but then also the less significant are the results it produces.

Nevertheless, it is a simple matter to derive the general τ/T relation for fully steerable telescopes, under the same assumptions on geographical and source locality as before. The total area of sky to be surveyed is given by Equation (4.25). If this is divided into n separate square areas, each has a side of about $\sqrt{4.87\lambda/n}$ radians (λ in meters). If the sum of these separate areas is to be scanned in a day, then the effective range in right ascension is the product of the number of areas, n, the number of scans per area $\Delta\delta/C_B \beta = \sqrt{4.87\lambda/n}/C_B \beta$, and the range in right ascension per scan $\sqrt{4.87\lambda/n}$. Thus the parameter n cancels (we might just as well have considered a single area given by Equation 4.25) and we have that in (slightly less than) 24 sidereal hours the effective right ascension range is $4.87\lambda/C_B \beta$. Thus if τ is the integration time spent when the beam β traverses a point source, then $\tau = 24 C_B \beta^2/4.87\lambda$ hours per day; thus in T days,

$$\tau = T\, 8.87 \times 10^3\, \beta^2/\lambda \text{ seconds},$$

where β is in radians, λ in meters. This then is an approximate but general expression for the τ/T relation for fully steerable telescopes, where there is no limit on T in this case. In terms of dish diameter for the fully steerable telescope we have therefore

$$\tau = T\, 1.44 \times 10^3\, \lambda/D^2 \text{ seconds} \tag{4.26}$$

which not surprisingly is the same as Equation (4.24) except that there are no (analytical) restraints on T or D.

The applicability of Equation (4.24) for almucantar antennas can be extended within the constraints of Equations (4.22) and (4.23e) on D and T. We have

$$D \geq \frac{4 C_\alpha \sqrt{C_C}}{1.55 \pi}$$

and

$$T \geq \frac{1.55 \pi D}{8 C_B}$$

i.e.

$$D \geq 300 \text{ meters}$$

and

$$T \geq 366 \text{ days},$$

for the parameters chosen in Equation (4.23b).

To summarize, the conditions assumed in Equations (4.23a and b) lead to

$$t = T \; 1.44 \times 10^3 \; \lambda/D^2 \text{ seconds} \tag{4.26}$$

for

$$0.3\text{m} \geq \lambda \geq 0.01 \text{ m} \tag{4.26a}$$

where for fully steerable telescopes

$$T \gtrsim 1 \text{ day} \tag{4.26b}$$

while for almucantar telescopes

$$T \geq 366 \text{ days}, \; D \geq 300 \text{ meters} \tag{4.26c}$$

A similar analysis can be made for smaller almucantar telescope diameters which may be considered in a later report.

5. Radiometric Considerations

5.1 Confusion Limit

We assume that source confusion arises when there is more than one point source

in C_C half-power beam areas $\omega^* = \pi\beta^2/4$, where we take the HPBW to be

$$\beta = 4\lambda/\pi D \qquad (5.1)$$

(λ is the wavelength and D the diameter of the dish in meters). Thus the total

number of sources in the sky that are separated in this way is $4\pi/C_C\omega^*$ and the number

per steradian is $N_C = 1/C_C\omega^*$. Thus we have for the number of sources per

steradian at the confusion limit

$$N_C = \frac{\pi}{4\,C_C} \left(\frac{D}{\lambda} \right)^2 \qquad (5.2)$$

For N_C to be as large as possible, D must be large and λ small, which are conditions

more easily realized for almucantar antennas than other single-dish designs. The

value of C_C is estimated to lie between 20 (Talen 1967) and 75 (von Hoerner 1961).

We choose $C_C = 50$, for which confusion problems in source counting are negligible.

(Shimmins, Bolton, Wall 1968)

5.2   Minimum Detectable Flux Density

The r.m.s. output noise temperature of a receiver is

$$\Delta T = \frac{C_s T_N}{\sqrt{\tau \Delta \nu}}$$

where T_N is the total system noise temperature equal to the receiver plus sky noise temperatures and is frequency dependent, τ is the integration time in seconds, $\Delta \nu$ the bandpass in Hz and C_s the sensitivity constant whose value depends on the type of receiver (Kraus, 1966, Table 7.3) and lies between 0.7 and 2.8. The minimum detectable flux density for point sources in flux units of 10^{-26} watts m^{-2} Hz^{-1} is

$$S_\nu = 10^{26} k \ \frac{4 \, C_s \, C_N}{\pi \, C_p \, C_A} \ \frac{T_N}{D^2 \sqrt{\tau \Delta \nu}}$$

where k = Boltzmann constant 1.380×10^{-23} joule/K, C_N is the signal/noise ratio whose value can be chosen in the range of say 5 to 10, $C_p = 0.5$ for non-polarized or randomly polarized light and $C_A \lesssim 1$ is the aperture efficiency. We let $\Delta \nu$ be the fraction $C_F \sim 0.05$ to 0.1 of the frequency ν and $C = 3 \times 10^8$ m sec^{-1} be the speed of light.

Thus

$$S_\nu = 10^{26}k \frac{4\,C_s\,C_N}{\pi\,C_p\,C_A\sqrt{C_F C}} \frac{T_N(\lambda)}{D^2}\sqrt{\frac{\lambda}{\tau}} \qquad (5.3)$$

We choose $C_s = 1.5$, $C_N = 7.5$, $C_A = 0.5$, $C_F = 0.1$; for purposes of comparison, our results are not much dependent on the precise values chosen. We let

$$10^{26}k\,\frac{4\,C_s\,C_N}{\pi\,C_p\,C_A\sqrt{C_F\,C}} = \kappa \qquad (5.4)$$

and we have in MKS units $\kappa = 14.36$. Flux densities for typical sources are shown diagramatically in Fig. 5.1. For the function $T_N(\lambda)$ adopted in Table 5.1, we assume maser noise temperatures of 50K and sky noise temperatures from the data of Drake (1960) and von Hoener (1961).

Table 5.1

λ(m)	0.003	0.005	0.008	0.012	0.015	0.02	0.03	0.1	0.3	1.0
ν(GHz)	100	60	37.5	25	20	15	10	3	1.0	0.3
T_N(K)	250	350	130	160	90	66	59	54	56	90

The most important property of Equation (5.3) for S_ν is the factor of 4 larger dependence in the exponent on D (the dish diameter) compared to τ (the integration time on a source). Thus if a telescope is designed in such a way that τ must be reduced by a factor of 100 say, then S_ν will be unaffected if the reduction in τ can somehow be translated into an increase in D by just a factor of $(100)^{1/4} \approx 3$. In the discussion of Section 3.5, we have seen how the time that a given point source is accessible to an almucantar antenna of fixed elevation is reduced by a factor of about 10^4 over that for a telescope that is essentially fully steerable, but is reduced by just a factor of only about 10^2 for an almucantar antenna with a very modest $\Delta Z = 1°$. Moreover, this factor becomes less as more realistic tasks are defined, such as source counting over

finite sky areas (Section 4.4), mapping of individual sources (Section 4.5.1) and of

the accessible sky (Section 4.5.2). The question is, therefore, whether a sufficiently

large dish with $\Delta Z = 1°$ can be designed to offset these reductions in observing time.

If so, and remembering from the discussion following Equation (4.5b) that an almucantar

antenna is at no disadvantage in sky survey work except insofar as the area of sky

covered is concerned, then an almucantar antenna has a decided advantage over fully

steerable telescopes, particularly at short wavelengths. Furthermore, even the

disadvantage of smaller sky coverage can be offset by suitable geographical spacing of

a number of similar telescopes whose unit cost should be reduced when more than one is

constructed. This in turn raises a number of interesting questions concerning the

possibility of interferometry between telescopes suitably spaced in both latitude and

longitude. Further discussion of these questions and a design proposal is found in

Chapter 6.

5.3 Sensitivity and time limits

The quest for the number of sources per steradian $N_s(S_\nu, \lambda)$ brighter than flux

density S_ν at wavelength λ, has motivated a great deal of observing and has produced

sometimes contradictory results. The major source of difficulty can be traced to the

problems of confusion in the interferometric source counts and edge effects, and how to

correct for them. Perhaps one major motivation for a pencil beam antenna is to check

the source counts found, for example, by the Cambridge one mile

interferometer (Pooley and Ryle 1968) and the single paraboloidal 210 foot Parkes telescope

(Shimmins, Bolton, Wall 1968) for which confusion errors are believed to be negligible.

Figure 5.2 shows the approximate behavior of the log N_s - log S_ν counts for the 2700

MHz Australian survey, the 408 MHz counts of Pooley and Ryle and the 178 MHz results

of Gower (1966) from the 4 C Survey, adapted from the data of those papers. The Pooley-Ryle results show a steeper slope of about - 1.8 and curvature towards smaller S_ν, whereas the Australian results have a flatter and constant slope of - 1.4. Before conclusions on cosmological models can be drawn from these results, it is necessary to disentangle any effect of evolution as it affects the spectral indices of the sources. This can be attempted when surveys are completed for as many wavelengths as possible, and to numbers of sources per steradian of

$$N \approx 10^5 \tag{5.5}$$

where cosmological model discrimination starts to be possible (e.g. Ringenberg and McVittie 1970).

The present state of flux concerning the log N_s - log S_ν relation suggests that we simply adopt an expression for $N_s(S_\nu, \lambda)$ that is appropriate to a Euclidean universe homogeneously filled with sources whose average spectral index is, say, $\alpha = 0.75$ (where $S \propto \lambda^\alpha$). In this case, the slope of the log N_s - log S_ν relation is -1.5 which lies within the range of values found at present. We have then for the number of sources per steradian limited to sensitivity S_ν in flux units

$$N_s = N_0 \left(\frac{\lambda}{\lambda_0}\right)^{\alpha n} S_\nu^{-n}, \tag{5.6}$$

where $\alpha = 0.75, n = 1.5$ (5.7a)

and, normalizing the formula to the 2700 MHz data of Shimmins et al (1968), we have

$$\lambda_0 = 0.11, \quad N_0 = 110. \tag{5.7b}$$

If we eliminate S_ν between Equations (5.6) and (5.3), we get the number of sources limited by time

$$N_t = \frac{N_o}{(\lambda_o^\alpha \kappa)^n} \left(\frac{\lambda^{(\alpha - 0.5)} D^2 \tau^{1/2}}{T_N} \right)^n \qquad (5.8)$$

5.4 Results for the Cosmological Problem

5.4.1 Optimum Wavelength and Aperture

Comparing Equations (5.2), (5.3) and (5.8), it is evident that the number of sources limited by confusion increases for decreasing λ, whereas the number limited by time or sensitivity increases for increasing λ, other things being equal. In general, a telescope is confusion limited at longer wavelengths and sensitivity limited at shorter wavelengths. The question arises as to the optimum operating wavelength as a function of dish size, time, and the defined task.

To evaluate this, we set

$$N_C = N_t \qquad (5.9)$$

and solve for T as a function of wavelength, dish size and task. For the task, we choose source counting in the cosmological problem, for which the τ/T relation is given by Equation (4.26).

Solving Equation (5.9) with the help of Equations (4.26), (5.2), (5.8), and (5.9) we have at the confusion limit

$$T = \left(\frac{\pi}{4 C_C N_o} \right)^{\frac{2}{n}} \frac{(\lambda_o^\alpha \kappa)^2 T_N^2 (\lambda)}{1.44 \times 10^3} \frac{D^{\frac{2}{n}(2-n)}}{\lambda^{\frac{2}{n}(2 + n\alpha)}} \qquad (5.10)$$

under the conditions (equations 4.26 a-c)

ART: $T \geq 366$, $\quad D \geq 300$ meters, $\quad 0.3 \geq \lambda$ meters ≥ 0.01.

With $n = 1.5$, $\alpha = 0.75$, $\lambda_o = 0.11$, $N_o = 110$, $\kappa = 14.44$, $C_C = 50$, we have

$$T = 3.94 \times 10^{-8} \frac{T_N^2 (\lambda) D^{0.667}}{\lambda^{4.167}} \qquad (5.11)$$

which is very sensitive to λ. The run of T versus λ is shown in Figure 5.3 for values of $T_N(\lambda)$ listed in Table 5.1, and as a function of D. The optimum λ is highly insensitive to D, and varies between 2 and 8 cm, depending slightly on the time available. Roughly speaking we can conclude that a telescope operating at wavelengths of maximum efficiency $\lambda \sim 2$ to 8 cm can be employed for the foreseeable future on the source counting problem.

5.4.2 Source counts

Substituting the τ/T relation for source counting from Equation (4.26) in the number of sources limited by time, Equation (5.8), we have

$$N_t = 5.61 \times 10^3 \left\{ \lambda^{1.125} / T_N^{1.5}(\lambda) \right\} D^{1.5} T^{0.75} \qquad (5.12)$$

while the number N_C limited by confusion is given by Equation (5.2). For almucantar telescopes this equation is applicable for $D \geq 300$ m, $T \geq 1$ year. For fully steerable telescopes on the other hand, D is limited by thermal, and gravitational deflection and stress considerations (von Hoerner 1967 and Chapter 6). We let the maximum value of D for a gravitational-deflection limited fully steerable telescope operating at wavelength λ be

$$D = 10^2 (\lambda/\lambda_K)^{1/2} \text{ meters.} \qquad (5.13)$$

where λ_K is a constant. When $\lambda_K = 0.053$ meters, von Hoerner's expression is

recovered; if the Bonn 100 meter telescope is efficient at 1.2 cm then λ_K could be as small as 0.012. For the FST case, Equation (5.12) gives

$$N_{t,\,FST} = 5.61 \times 10^6 \, \lambda^{1.875} \, T^{0.75} \, / T_N^{1.5}(\lambda) \, \lambda_1^{0.75} \tag{5.14a}$$

while for the almucantar case,

$$N_{t,\,ART} = 5.61 \times 10^3 \, D^{1.5} \, \lambda^{1.125} \, T^{0.75} \, / T_N^{1.5}(\lambda) \,, \quad (D \geq 300 \text{ m}) \tag{5.14b}$$

Similarly, expression (5.13) gives for the confusion limit (5.2):

$$N_{C,\,FST} = 1.57 \times 10^2 / \lambda \lambda_1 \,, \tag{5.15a}$$

while for the almucantar telescope

$$N_{C,\,ART} = 1.57 \times 10^{-2} \, D^2 / \lambda^2 \,. \tag{5.15b}$$

The functions (5.14)-(5.15) are plotted in Figure (5.4) for $D_{ART} = 300$ m and the value $\lambda_1 = 0.053$ as given by von Hoerner (1967). The figure shows that as λ decreases from about 50 cm, the almucantar telescope with $D = 300$ m, outperforms the largest fully steerable dish by ever increasing numbers of sources, reaching a factor of about 6 more at the optimum wavelength limit at $N_C = N_t$, and up to a factor 20 more at millimeter wavelengths. The time limited curves have been drawn for $T = 1$ year, and can be scaled upward according to the factor $T^{0.75}$ in Equations (5.14) and (5.15) if longer observing times are sought. Similarly, other values of $D > 300$ m and of λ_1 can be used in equations (5.14-5.15).

The actual number of sources observed, n, is the product of the numbers per steradian and the solid angle in Equation (4.25). These are shown in Figure 5.5 for the cited conditions. It is seen that the λ-dependence in the confusion limit $n_{C,\,FST}$ cancels, leading to the horizontal line in Figure 5.5. This figure shows that statistically meaningful numbers of sources can be counted in 1 year for

wavelengths longer than about 1 or 2 cm, for the chosen cosmological model. Once again, upward scaling by $T^{3/4}$ can be done for longer project times.

Both Figures 5.4 and 5.5 show the great desirability of large receiving areas at short wavelengths, where source counts are time limited. It is precisely at centimeter and the longer millimeter wavelengths that almucantar radio telescopes should demonstrate their greatest superiority. Note further that it becomes increasingly difficult to achieve the limit (5.13) for fully steerable telescopes, whereas the value of D for the almucantar case can be increased well beyond this limit (see Chapter 6).

5.4.3 Source Monitoring

The study of the variability of quasi-stellar radio galaxies in both radio and optical wavelengths is important for an understanding of the nature and evolution of these objects (see e.g. Pacholczyk and Weymann 1968) and hence also for the solution of the cosmological problem. The radio flux of the Seyfert galaxy 3C120, for example, varies by up to a factor of 3 at wavelengths between 2 and 10 cm (Pauliny-Toth and Kellerman 1968) which may be correlated with variability on a similar time scale at optical wavelengths (Usher, 1972). Thus it behoves us to investigate the capabilities of ART and FST designs in monitoring quasi-stellar sources, due to their cosmogonical significance to cosmology.

The FST design is superior insofar as such a telescope can track one source for extended periods of time in a day, and can reach a greater number. This must be weighed against the advantage of the ART design with shorter observing times but which can be built with larger aperture. The question, therefore, devolves once again to a trade-off between τ and D in Equation (5.3). Let us assume that the source position is well enough known that a single scan of the source is sufficient, and that we observe only sources very much brighter than the confusion limit. The minimum detectable flux at the confusion limit is found by solving the equation $N_C = N_s$ for S_ν by use of Equations (5.2) and (5.6). We have

$$S_\nu = \left(\frac{N_o}{\lambda_o^{\alpha n}} \; \frac{4 C_C}{\pi} \; \frac{\lambda^{2+\alpha n}}{D^2} \right)^{\frac{1}{n}}$$ (5.16)

whence at $\lambda = 3$ cm it follows that

$$D^2 S_\nu^{3/2} = 1.47.$$

This is the dashed line plotted in Figure 5.6. To find the minimum detectable flux limited by time, we substitute the appropriate expression for τ into Equation (5.3). From Section 4.3 (Equations 4.8 and 4.9) we have for a source at the equator

$$\tau = 2 \beta_t \left(1 + \frac{\Delta H}{\Delta \alpha} \right)$$ (5.17)

where we recall that ΔH is the hour angular duration of the observing time on one or the other side of the meridian, and where we have taken $C_{EW} = 2$ in order to give two scans over the source per day (This implies a time resolution for variability of less than or about a day; a similar analysis would pertain for finer time resolution for which the almucantar design has a clear advantage due to its greater collecting area and because it becomes less hampered by its limited elevation steerability as smaller time resolution is demanded).

For purposes of relative radiometry we take

$$\Delta \alpha = 8 \beta = \frac{32}{\pi} \frac{\lambda}{D}.$$ (5.18)

where $8 \approx \sqrt{C_C}$ is a little greater than the diameter of the area in which sources are not confused (see Section 5.1). For ΔH we choose the values listed in Table 5.2 which cover the possibilities for an ART design of $\Delta Z = 1°$ (i.e. $\Delta H \leq 4$ min, on either side of the meridian at the equator) and an FST design for tracking above a zenith angle of 60° (i.e. $\Delta H \leq 4^h$)

Table 5.2

ΔH (λ me)	ΔH (rad)	Design applicability to
4^{sec}	$\pi/18000$	ART, FST
24^{sec}	$\pi/3000$	ART, FST
4^{min}	$\pi/300$	ART, FST
40^{min}	$\pi/30$	FST
4^{hours}	$\pi/3$	FST

From Equations (5.15), (5.16) and (5.4), the expression (5.3) for the minimum detectable flux in flux units as a function of D in meters becomes at λ = 3 cm

$$S_\nu = \frac{4.55}{D^2 \sqrt{\dfrac{1}{D} + 3.27 \, \Delta H}}$$

(5.19')

which is plotted in Figure 5.6 for values of ΔH given in Table 5.2.

Figure 5.6 once more demonstrates the superiority of the ART design. Compare for example the minimum detectable flux S_ν at the FST limit, with a 300 meter ART design, both at the confusion limit. S_ν is smaller for the ART design by nearly an order of magnitude, requiring 24 seconds of observing time compared to 4 minutes for the FST design. This implies also that up to about a factor of 10 more sources can be monitored by the almucantar telescope in the same time.

Needless to say, the superiority of the almucantar telescope design is once again a consequence of the fact that dish diameter is more important than integration

time by a factor of 4 in the   exponent, in reducing the minimum detectable flux.

The almucantar design is at a disadvantage however, if absolute flux measurements

of variable sources is required, unless standard sources are readily available in

the sky, or unless a reliable internal calibration source is available. Nevertheless,

standard celestial sources are a sine qua non for absolute radiometry, whatever

type of telescope is being used.

5.5 Miscellaneous Considerations

We have evaluated the relative capabilities of ART and FST designs under

the assumption that a single on-axis receiver is used. It is conceivable that off-axis

receivers can be used, but this consideration is not taken into account because it

would not affect the relative performances of the two types of telescopes.

There are two considerations along these lines that should be mentioned however.

The first is that the ART design has the unique and desirable feature (as was pointed

out originally by Usher 1963) that the focus tower can be built directly upon the ground

(see Chapter 6 concerning a preliminary design proposal). Thus if a Cassegrain system is

used or even if the prime focus is used, the installation of a multiple feed system

is more easily accomplished for ART designs since, one way or another, heavy

equipment at the focus rests directly on the ground and does not cause unnecessary

gravitational distortions of the dish.

The second consideration is that increasing the number of off-axis receivers

decreases the time necessary to reach the confusion limit. Thus the time T can be

replaced in the above equations by rT' where r = number of receivers. The full

implications of this need working out, but qualitatively the effect would be to move to

shorter wavelengths in Figure 5.4 and 5.5 the point where $N_t = N_c$ for reasonable

observing times. Thus multiple off-axis receivers are more urgently needed at centimeter and millimeter wavelengths.

Finally we note that the dependence of the minimum detectable flux $S_\nu \sim D^{-2} (\tau \, \Delta\nu)^{-1/2}$ on diameter D, integration time τ and bandwidth $\Delta\nu$ is such that a decrease in $\Delta\nu$ for spectral line work can be compensated more effectively by an increase in D rather than an increase in τ.

6. A Preliminary Design Proposal

The results of Chapter 5 have shown the greater importance of dish size compared to dish steerability for source monitoring and the cosmological problem. We have seen how some degree of steerability is desirable to achieve some flexibility in the use of the telescope. The question arises as to how these goals might be achieved and the mechanical limitations and cost-effectiveness of the different possibilities. The discussion here is by necessity of a qualitative yet heuristic nature.

von Hoerner (1967) has spelled out the natural limits (as against economical limits) of a telescope. These are

1) Gravitational deflections

$$D_g = 100(\lambda/5.3 \text{ K})^{1/2} \qquad\qquad (6.1)$$

(D in meters, λ in cm) for telescopes tiltable through $Z = 90°$ with

K $\sim$ 1.2 to 1.8

2) Bearing stress limit

$$D \sim 600 \text{ meters} \qquad\qquad (6.2)$$

for large ΔZ.

3) Thermal deflections

$$D_t = 100 (\lambda/2.4) \qquad\qquad (6.3)$$

for temperature differences of $\sim 5°C$.

4) Wind deflections

$$D = 100 (\lambda/7.5) \qquad\qquad (6.4)$$

for survival conditions

5) Maximum height limit

$$h \sim \begin{cases} 1790 \text{ meters for steel} \\ 3370 \text{ meters for aluminum} \end{cases} \tag{6.5}$$

The first two limits are beaten by the ART design, the first because the

telescope is not tilted. Therefore the second limit is overcome because there are

no bearings; the telescope weight is distributed over the ground without being vectored on

the bearings of the tilt axis. How a $\Delta Z \gtrsim 1°$ can be achieved will be discussed shortly.

The next two limits are beaten beaten by enclosing the structure in a radome or its

equivalent. Even so, a thermal gradient can exist, but this can be effectively eliminated

by forced air conditioning. Alternatively, an environmental telescope can be designed

to undergo homologous deformations under varying ambient temperatures (diurnal and

season) thus preserving its focusing properties, and its use would then be restricted

to low wind velocities.

We conclude that the only natural limit that exists for the ART design is the

last, which sets a limit on the maximum height that a structure can reach. For the

ART design, this is

$$D = h \operatorname{cosec} Z_{MAX} \tag{6.6}$$

or from Equation (6.5) for $Z_{MAX} = 30°$

$$D = \begin{cases} 2580 \text{ meters for steel} \\ 6740 \text{ meters for aluminum} \end{cases} \tag{6.7}$$

These values are so large that they approach the separations of the Cambridge,

England one-mile interferometer. (In fact the limits of Equation (6.7) can be

increased even more by such schemes as filling the structural members with helium.)

The preceding discussion does not presume to suggest that a telescope of this

size be built. Rather it points out that there is effectively no limit to the size of an

almucantar antenna short of its maximum height.

We consider next the question of the radome and how $\Delta Z \sim 1°$ (say) can be achieved—that is additional to any ΔZ obtained by moving the feed.

In ART designs, the large diameters and the basic tilt of Z_{MAX} is achieved by converting the entire support structure from an active to a passive role, and a degree of steerability is superposed as a perturbation (as it were) by introducing a a movable surface structure which will accomplish the steering in elevation. One can imagine, for example, coupled extensible rods, strong enough in a radome merely to support their own weight and that of the antenna surface, and resting upon the gross passive infra-structure; this in turn rests directly on circular azimuthal tracks on the ground to accomplish the desired steering in azimuth. In fact, such a design would also enable the surface tolerance to be maintained to the 67% efficiency predicted by the Ruze formulae (Ruze 1966) at $\Delta\lambda \sim \lambda/10$, under whatever environmental conditions might exist. (It is appropriate to note that one can also rely on this form of active compensation to maintain surface tolerance in the absence of a radome.) Moreover the use of active compensation is most suitable for the antenna under discussion here (see e.g. Rothman and Chang 1969) because of the large structural size (for which homology methods for fully steerable telescopes may be either uneconomical or impossible) and because the telescope can be non-environmental (see the discussion of a radome below). The amount by which the extensible rods must extend should be at most about $D \Delta Z$, or about 500 cm for a 300 meter telescope with $\Delta Z = 1°$. For use at wavelengths of 8 mm, the tolerance on the compensating elements would have to be less than about 1 mm. or about one part in 5000. Through the use of such a low mass active compensation surface, accurate source location should be possible.

The basic geometric simplicity of the ART design argues strongly in favor of a radome, for two reasons. The first concerns the nature of the focus mount. As we pointed out some years ago, a telescope fixed in elevation (or clearly also one with limited steerability in elevation) can be designed with a focus tower built directly upon the ground, thus not only freeing the surface support structure from its distorting loads, but also enabling the azimuthal rotation to occur about it. In a radome enclosure, the focus mount can then also serve (if necessary) as a means of supporting the radome in the center, thereby enabling it to be larger in size. Concerning the nature of the focus tower, it is clear that, just as the telescope has a gross passive and small active structure, so the focus tower must have the same properties, the active part being steerable to the same degree that the telescope is steerable.

The second advantage of the natural simplicity of the ART design is that the greater part of the radome can consist of the earth itself, since only those solid angles in the sky that the telescope is designed to reach need be transparent to radio waves. It seems entirely reasonable to suggest, therefore, that the telescope be built in a hole in the ground where the earth protects it from wind and in which a temperate environment is more easily maintained.

For reasons both mechanical and optical, a Cassegrain system is the preferable design. A tiltable secondary mirror returns the converging beam to the base of the telescope where it is more accessible, virtually fixed in position, and where heavy equipment can be placed with impunity. Several options exist for the support of the secondary; either it can be supported by a focus tower built directly on the ground, or it can be suspended by cables in much the same manner as the prime focus feeds are supported at Arecibo, thereby minimizing shadowing on the main reflector.

Further advantages of a Cassegrain design have been spelled out by Christiansen and Högbom (1969). With double mirror optics the focal ratio can be increased to say f/1 or f/2 with a resultant suppression of coma in off-axis images. This allows an increase in the number of receivers and consequently an increase in observing efficiency. The full capacity for steerability in elevation can also be ascribed to motion of the feed through the error-free field. The use of a Gregorian elliptical secondary rather than a hyperbolic secondary protects the prime focus from extraneous lateral radiation. Also the secondary focus feed points towards the sky which is cold at short wavelengths, whereas a prime focus feed would point towards the ground which is hot. In addition, the greatly enhanced ability of the almucantar design to minimize deflections in reflecting surfaces is just what is required for multiple reflecting systems such as a Cassegrain telescope.

Finally, we must deal with the only apparent advantage of a fully steerable telescope over an almucantar design, viz., its ability to reach a greater fraction of the sky. For small D, the cost (it is believed) goes as D^3 for a fully steerable telescope, whereas it should go more like D^2 for an almucantar design. But as D increases, and as the natural limits on FST telescopes are approached, exponential factors arise which send cost $\rightarrow \infty$, whereas the D^2 dependence should remain for the almucantar telescope well past these limits. Almucantar telescopes are economically justified not only for this reason however. A second practical article of faith among economists is that mass production lowers the unit cost. So if this be true, the cost of sky coverage for almucantar antennas should go as nD^α where n = number of telescopes, and where α is probably ≈ 2 when the cost of the active steering mechanism in altitude is reckoned with. Whatever the precise form of this dependence, the fact is that the basically simple geometry of an almucantar antenna

system allows one to achieve complete sky coverage with a high resolution coherent beam at a cost that does not approach infinity, but rather increases linearly with the cost of a basically inexpensive unit. Furthermore, the payoff (in terms of observational results) is immediate for source monitoring, source location and source identification, by the almucantar telescope whereas for source counting to cosmologically significant levels, the payoff comes after longer periods of time. Yet as time goes by, the value of the results in the wavelength range considered are incomparably better than those obtained after equal effort by the largest feasible fully steerable telescope. Objectively speaking it is hard to argue at this point with the apparent conclusion that almucantar telescopes should provide possibly the greatest return for the least investment of capital.

7. Concluding Remarks

We have made a preliminary evaluation of a highly complex and multi-parametric problem, and clearly much work remains to be done. To begin with, the formulations and calculations in this report need to be expanded to cover all reasonable parametric combinations, and secondly, an engineering study should be initiated to evaluate the mechanical problems. Other aspects that need exploration are: (i) explore the possibility of interferometry by almucantar (and other) antennas spaced appropriately in latitude and longitude; (ii) work out the details on slew rates and tilt rates; (iii) evaluate the telescope's use as a radar instrument; (iv) determine the affect of multiple off axis receivers.

In conclusion, we feel

(1)   that the case for the almucantar antenna has been adequately demonstrated, but that much work remains before a final verdict can be reached;

(2)   that just as the concept of homology utilizes nature to advantage in solving the problem of the small telescope, so the almucantar design avoids brute-force methods, and employs nature to full advantage for all telescopes, large or small;

(3)   that an almucantar telescope system is cost-effective;

(4)   that almucantar telescopes employ the tested capabilities of present technology and need not necessarily go through prototype and development stages as would be the case, for example, with homology telescopes;

(5)   that the solution for the best high gain telescope cannot be found until the almucantar telescope is thoroughly evaluated.

8. Acknowledgements

It is a pleasure to thank Professor John P. Hagen for his enthusiasm and encouragement to pursue this project, and to Drs. Hagen, Frank Zabriskie and Paul Swanson for critically reading the manuscript. I am especially indebted to Professor Paul Ebaugh for his support. I also wish to express my gratitude to Miss Laura K. Hutton for assistance with some of the numerical work.

9. References and Bibliography

Cambridge Radio Observatory Committee "A Large Radio-Radar Telescope; Camroc Design Concepts", Vols. I, II, 1967.

Chauvenet, W., 1863, "A Manual of Spherical and Practical Astronomy" Vol. 1, Dover Publications Inc. 1960.

Christiansen, W. N., Högbom, J. A., 1969 "Radiotelescopes" Cambridge University Press.

Drake, F. D., 1960 "Radio-Astronomy Radiometers and Their Calibration" Stars and Stellar Systems, University of Chicago Press, Vol. 1, p. 210.

Findlay, J. W., 1971 "Filled-Aperture Antennas for Radio Astronomy" Advances in Astronomy and Astrophysics 9, 271.

Gower, J. F. R., 1966 "The source counts from the 4C Survey" Mon. Not. Royal Ast. Soc. 133, 151.

Kraus, J. D., 1966 "Radio Astronomy" McGraw-Hill Co.

Mar, J. W., Liebowitz, H., editors "Structures Technology for Large Radio and Radar Telescopes Systems" MIT Press 1969.

North American Aviation, Inc., 1963 "Design Description of 600-foot Radio Transit Telescope".

Northeast Radio Observatory Committee "A Large Radio-Radar Telescope; Engineering Studies" Vols. I, II, 1968.

Pacholczyk, A. G., Weymann, R., editors "Proceedings of the conference on Seyfert Galaxies and Related Objects" Astronomical Journal 73, 836, 1968.

Pauliny-Toth, I. I. K., Kellermann K. I., 1968 "Repeated Outbursts in the Radio Galaxy 3C120" Ap. J. Letters 152, L169.

Pooley, G. G., Ryle, M., 1968 "The Extension of the Number-Flux Density Relation for Radio Sources to Very Small Flux Densities" Mon. Not. Royal Ast. Soc. 139, 515.

Ringenberg, R., McVittie, G. C., 1970 "The Evolution Function and the Interpretation of Radio Source-Counts" Mon. Not. Royal Ast. Soc. 149, 341.

Rothman, H., Chang, F. K., 1969 (see Mar and Liebowitz 1969).

Ruze, J. 1966 "Antenna Tolerance Theory-A Review" Proc. I.E.E.E. 54, 633.

Shimmins, A. J., Bolton, J. G., Wall, J. V., 1968 "Counts of Radio Sources at 2700 MHz" Nature 217, 818.

Talen, J. L. 1967 "Capabilities of a Fixed Elevation Antenna" University of Michigan, Radio Astronomy Observatory, Ann Arbor, Michigan.

Usher, P. D., 1963, "Radio-Transit Telescopes Steerable in Azimuth" Nature 197, 170.

Usher, P. D., 1971 "Capabilities of Almucantar Radio Telescopes" Paper presented to the 136th Meeting of the American Astronomical Society, San Juan, Puerto Rico, 6-8 December.

Usher, P. D., 1972 "The Case for Correlated Optical and Radio Variability of the Seyfert Galaxy 3C120" Ap. J. Letters, 172, L25.

von Hoerner, S., 1961 "Very Large Antennas for the Cosmological Problem 1 Basic Considerations" Publ. Nat. Rad. Ast. Obs. 1, No. 2.

von Hoerner, S., 1967 "Design of Large Steerable Antennas" Astronomical Journal 72, 35.

10. Personnel, etc.

In addition to the principle investigator this sub-grant supported part-time a student, Miss Laura K. Hutton, who was initially an undergraduate major in Astronomy, and prior to her graduate studies in Astronomy at the University of Maryland was a summer assistant. The major results of this work were presented at the 136th meeting of the American Astronomical Society in San Juan, Puerto Rico (Usher 1971).
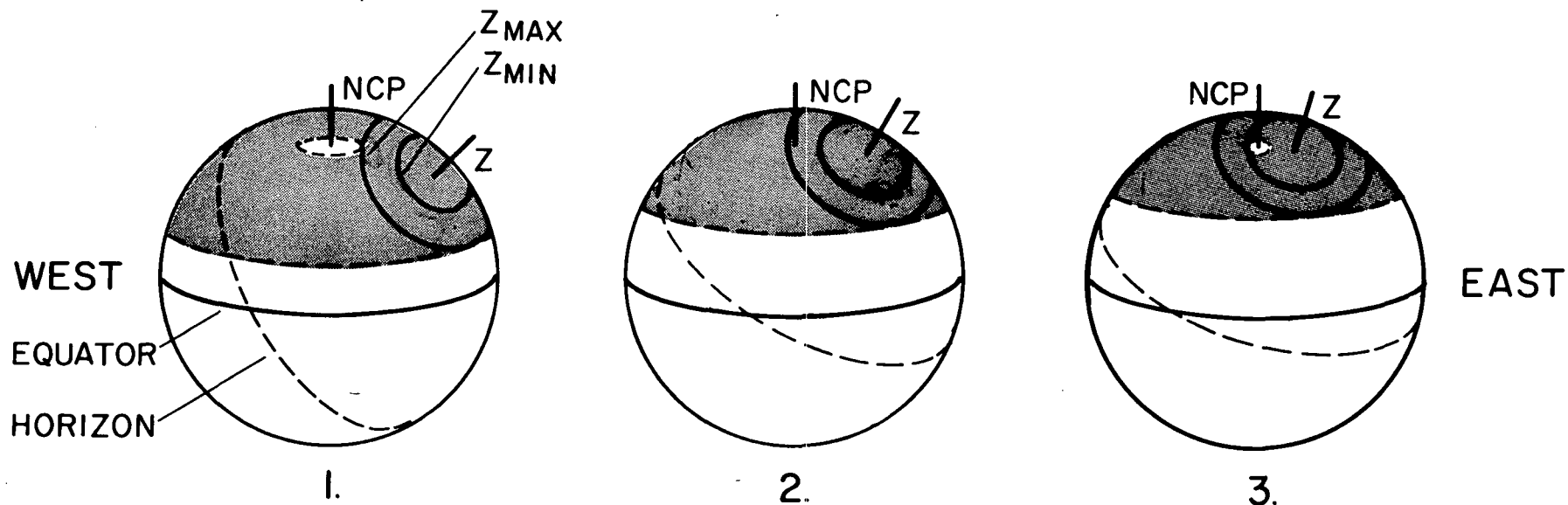
Figure 2.1

Celestial sphere showing the three cases described in the text i.e.,
as the latitude of the observer increases, the north celestial Pole
falls (1) completely outside both the almucantars, or (2) between
them or (3) completely inside both. Sources lying within the shaded
area are accessible to observation on both sides of the meridian.
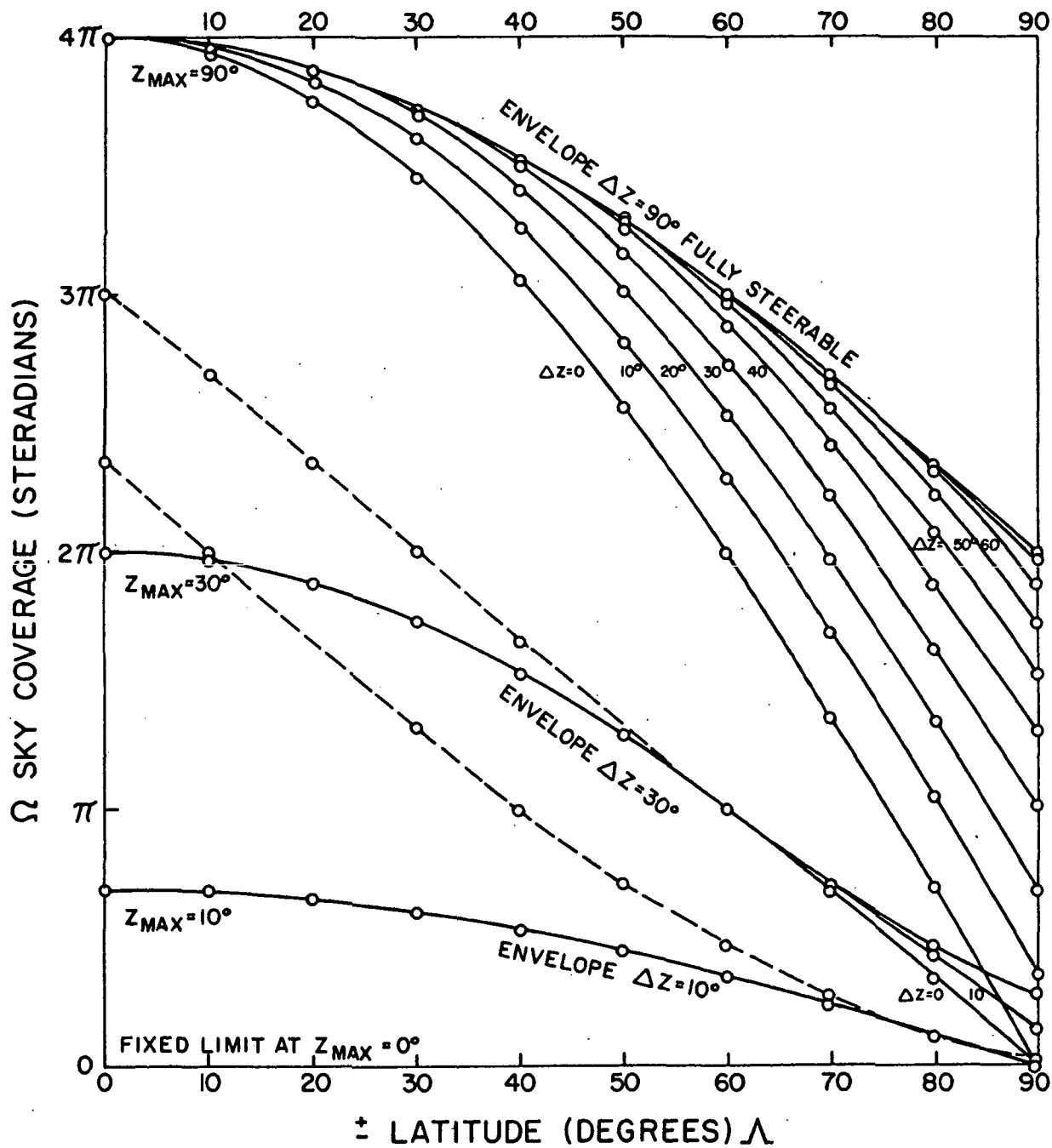
Figure 2. 2a

Sky coverage for an infinitesimal beamwidth and partially and fully steerable
antenna, as a function of geographical latitude. See Figure 2. 3 for aid in reading.
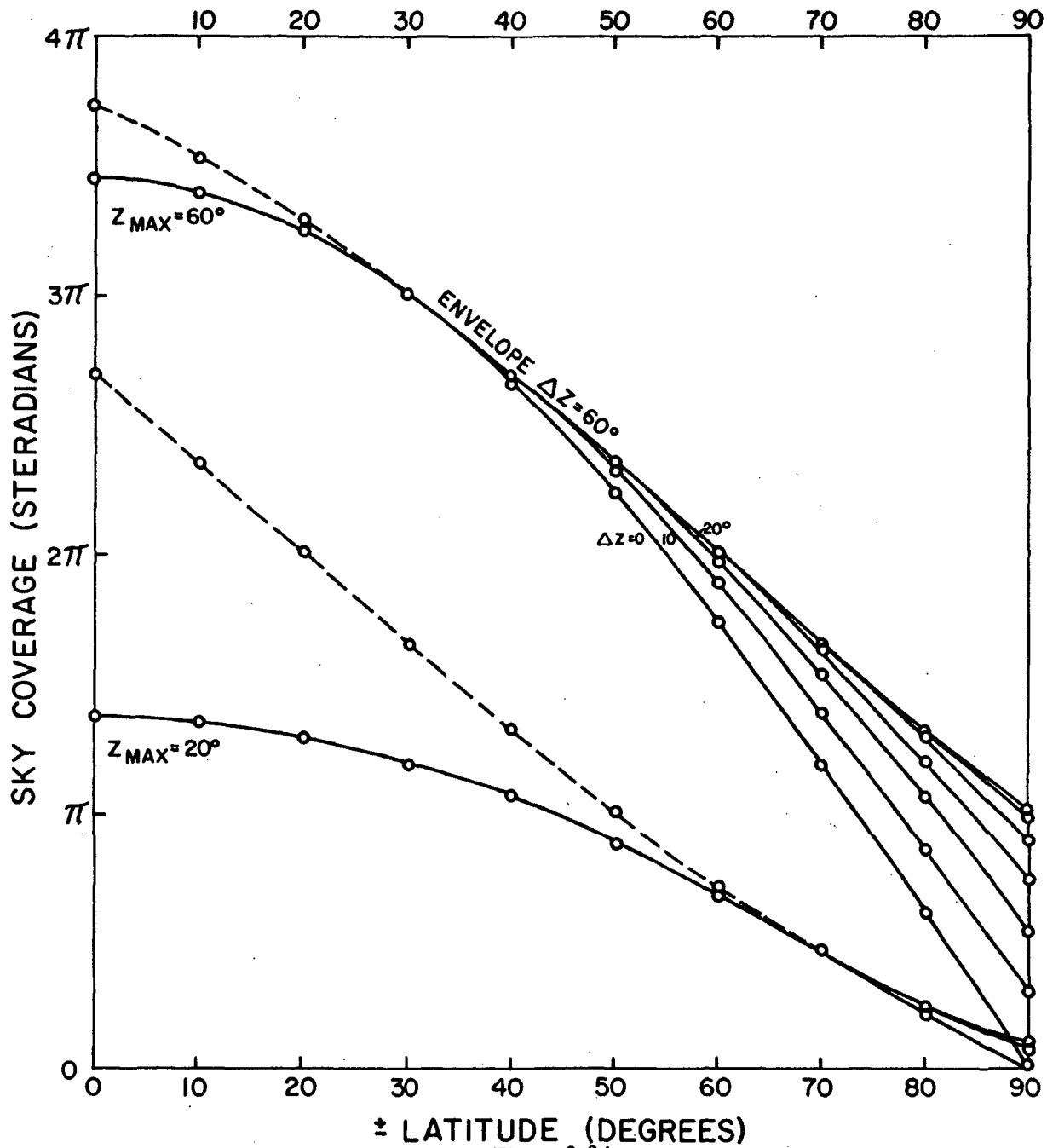
Figure 2.2 b

Sky coverage for an infinitesimal beamwidth and partially and fully steerable
antenna, as a function of geographical latitude. See Figure 2.3 for aid in reading.
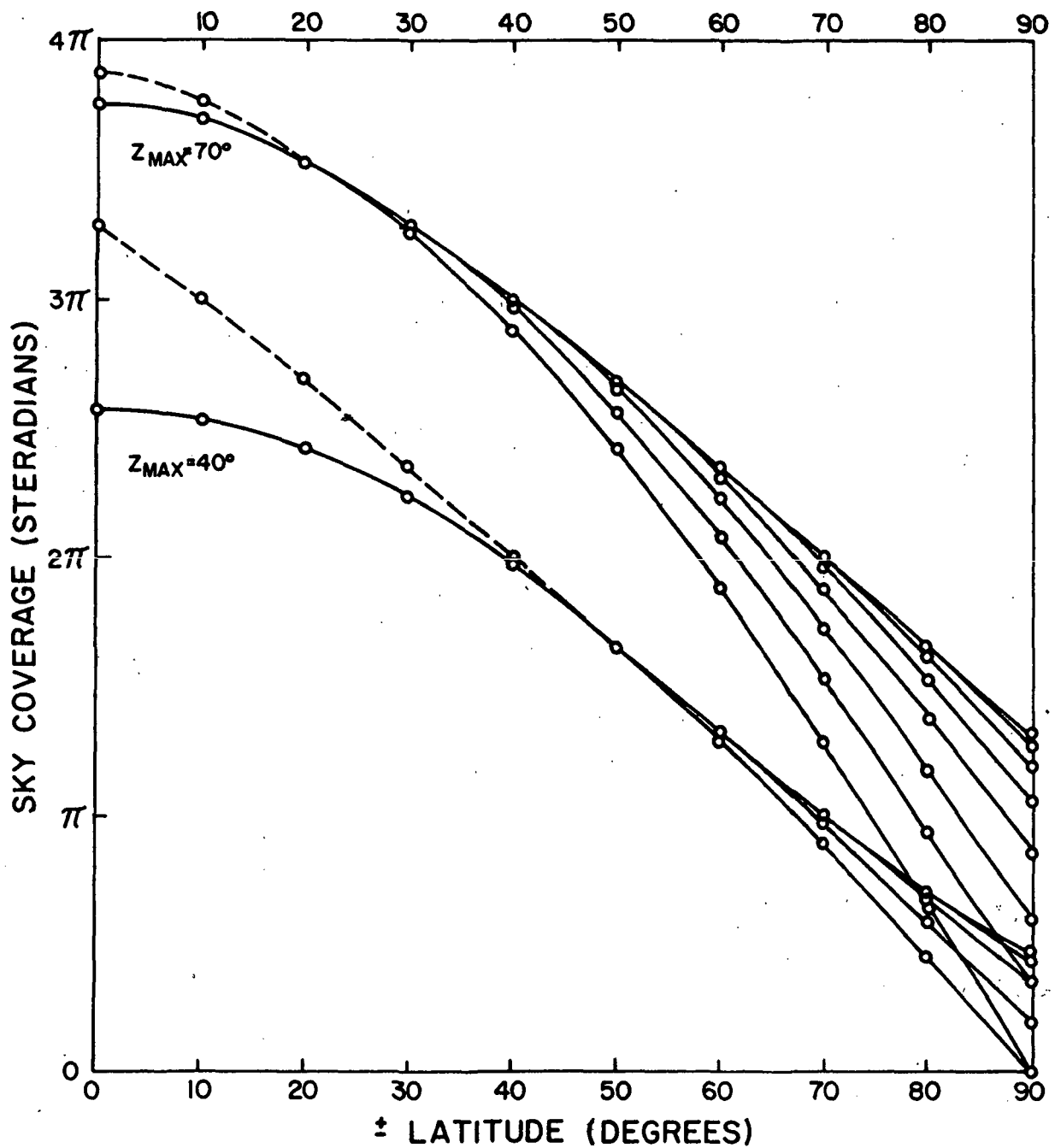
Figure 2.2c
Sky coverage for an infinitesimal beamwidth and partially and fully steerable
antenna, as a function of geographical latitude. See Figure 2.3 for aid in reading.
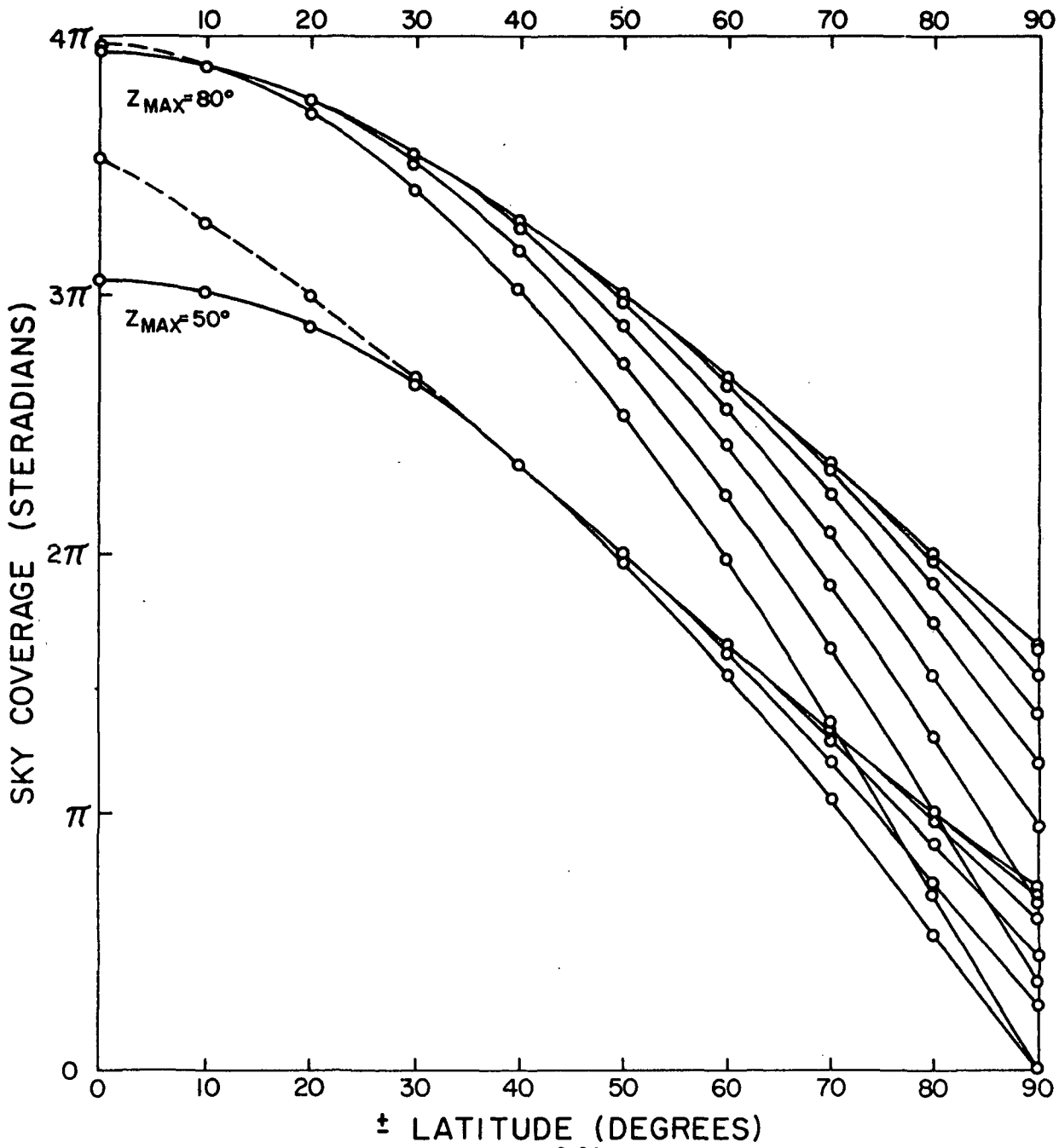
Figure 2.2d
Sky coverage for an infinitesimal beamwidth and partially and fully steerable
antenna, as a function of geographical latitude. See Figure 2.3 for aid in reading.
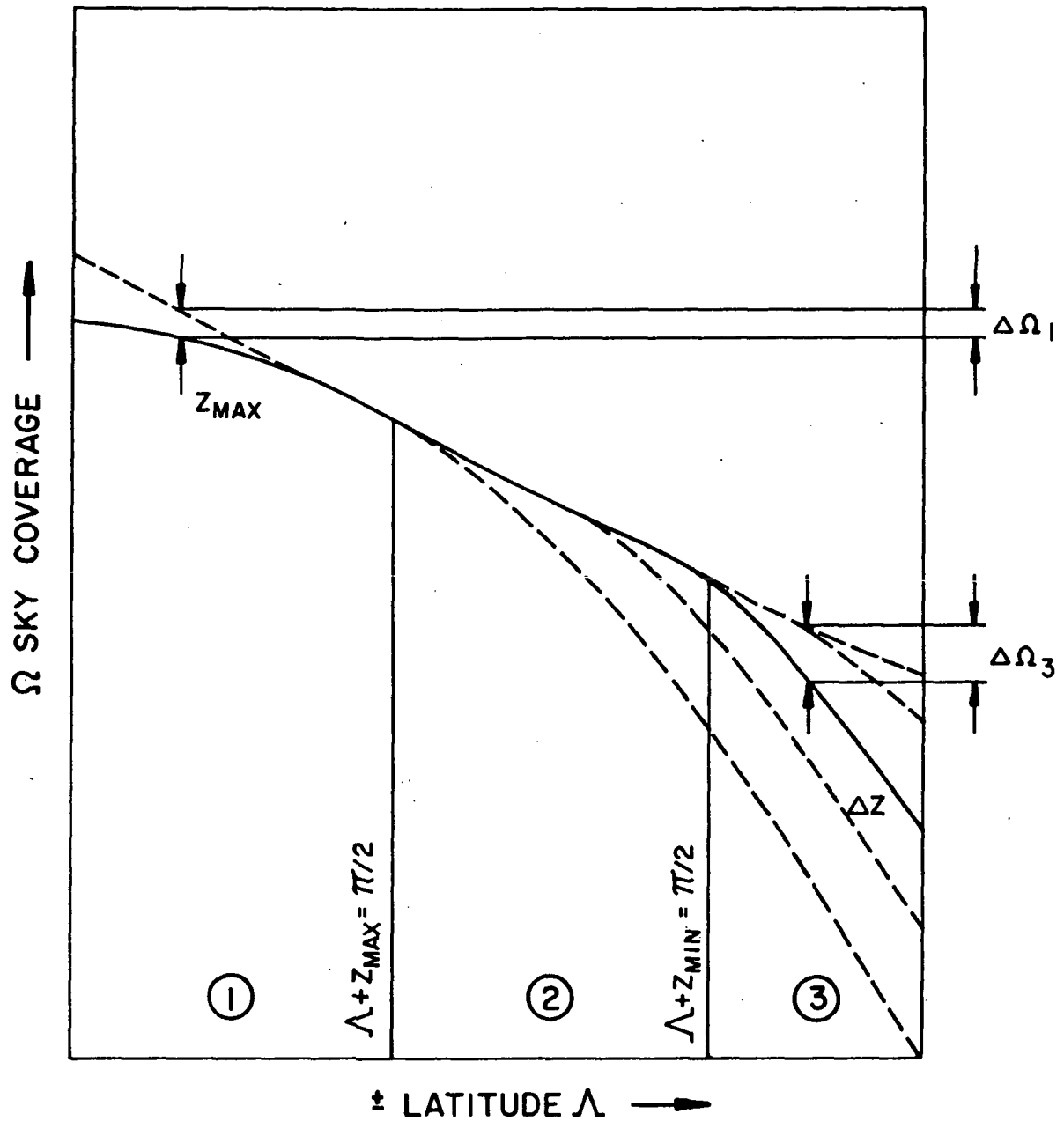
Figure 2.3

Schematic representation of the family of curves in Figures 2.2(a-d) for given Z_{MAX} and Z_{MIN}, showing the zones 1, 2 and 3 in which cases 1, 2, and 3 of Equation (2.1) are applicable. Also shown are the inaccessible circumpolar solid angles $\Delta\Omega_1$ in case 1 and $\Delta\Omega_3$ in Case 3.
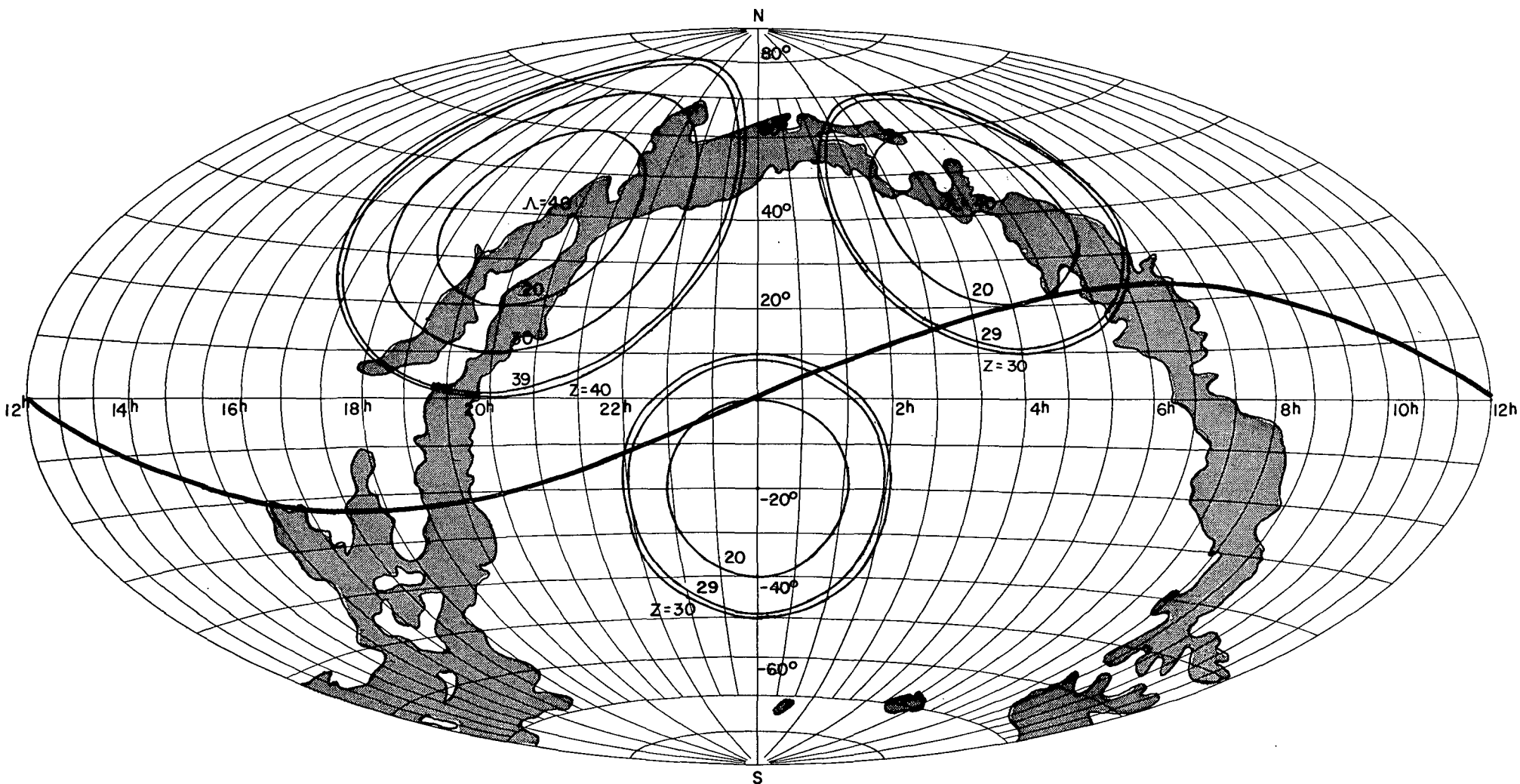
Figure 2.4

Aitoff equal area projection of celestial sphere, showing the
instantaneous sky coverage for the cases $\Lambda = 40°$, $Z_{MAX} = 30°$
and $40°$, and $\Lambda = -20°$ with $Z_{MAX} = 30°$. Also shown is the
Milky Way, the Magellanic Clouds and the ecliptic. Coordinates
are right ascension in hours, declination in degrees.
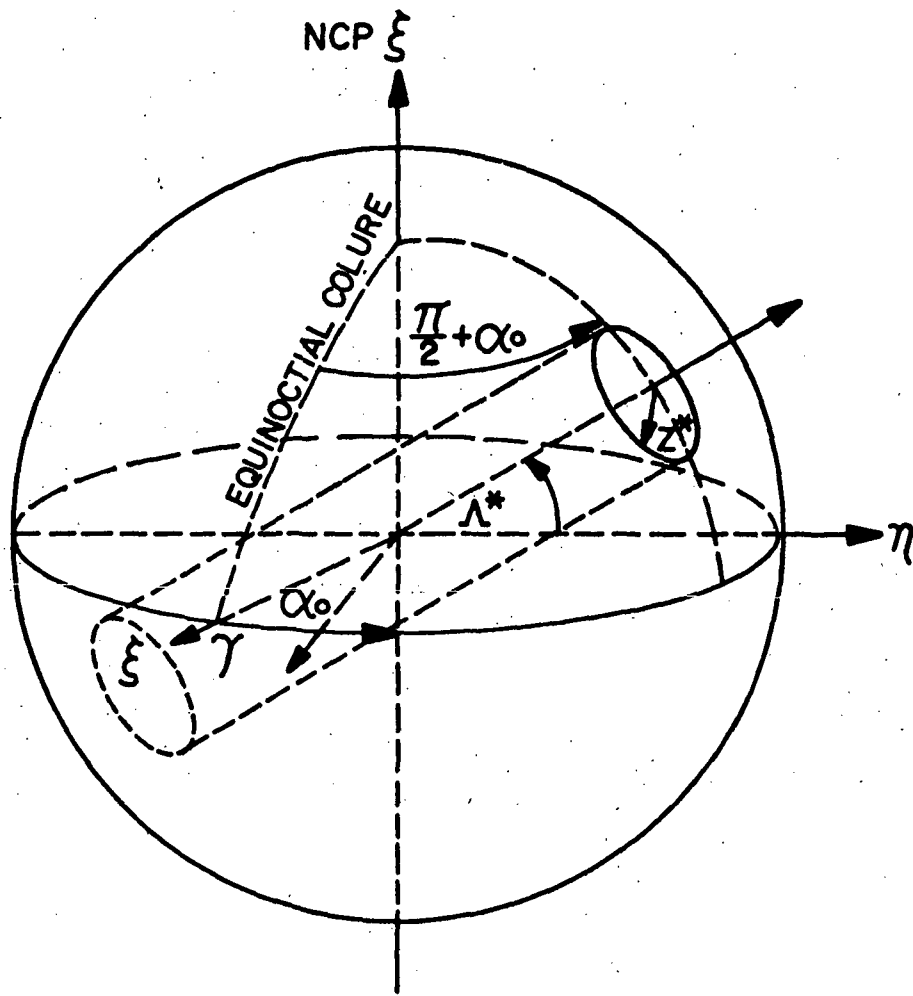
Figure 2.5

Parameters defining the position and size of a
general small circle on the celestial sphere.
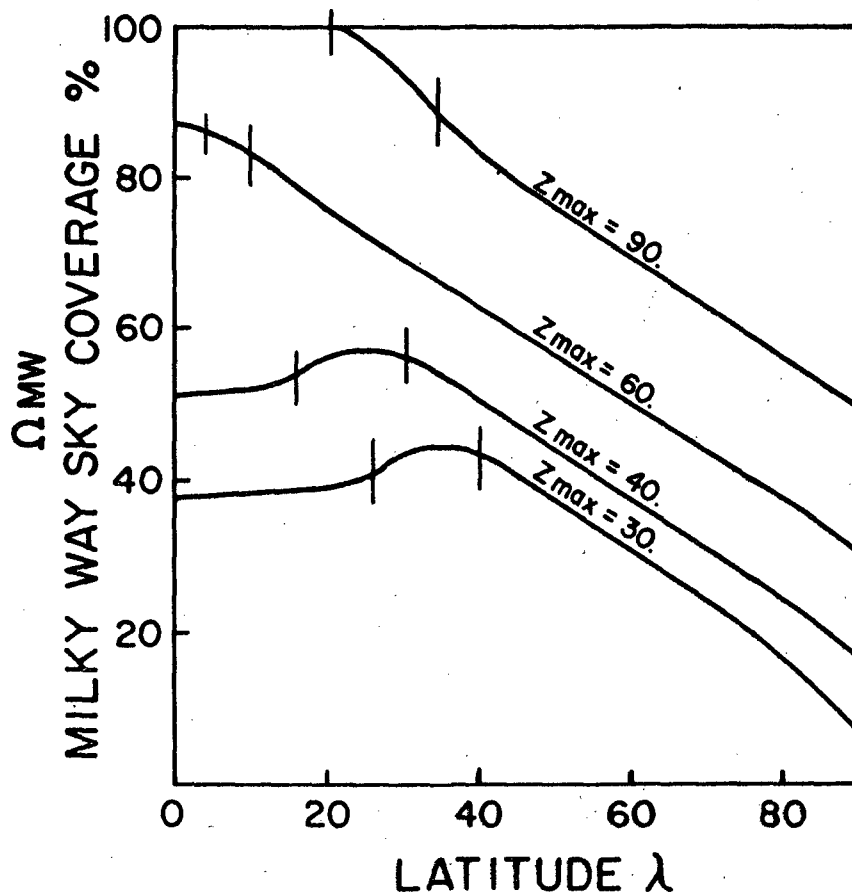
Figure 2. 6

Milky Way sky coverage as a function of geographical latitude for $Z_{MAX} = 30°$, 40°, 60° and 90°. On the curves for $Z_{MAX} = 30°$, 40° and 90° the first discontinuity (indicated by a vertical line) represents the latitude at which the highest declination reached by the telescope just passes the most northerly point of the southern edge of the Milky Way. The second discontinuity represents the latitude at which the highest declination reached passes the northern edge of the Milky Way. The maxima are due to the relatively large area which is added in the north between these points. On the $Z_{MAX} = 60$ curve the first discontinuity represents the most southerly declination reached passing the southernmost point of the northern edge of the Milky Way, while the second discontinuity represents the northernmost declination passing the northern edge.

$$\delta = \Lambda + Z_{MAX}$$

$$\delta = \Lambda + Z_{MIN}$$

$$\delta = \Lambda$$

SOURCE DECLINATION

$$\delta = \Lambda$$

CELESTIAL EQUATOR $= 0$

$$\delta = \Lambda - Z_{MAX}$$

HORIZON $Z = 90°$

MERIDIAN

H_{MAX}

H_{MIN}

NCP

Z

S_2 S_1

Z_{MAX}

Z_{MIN}

WEST | EAST
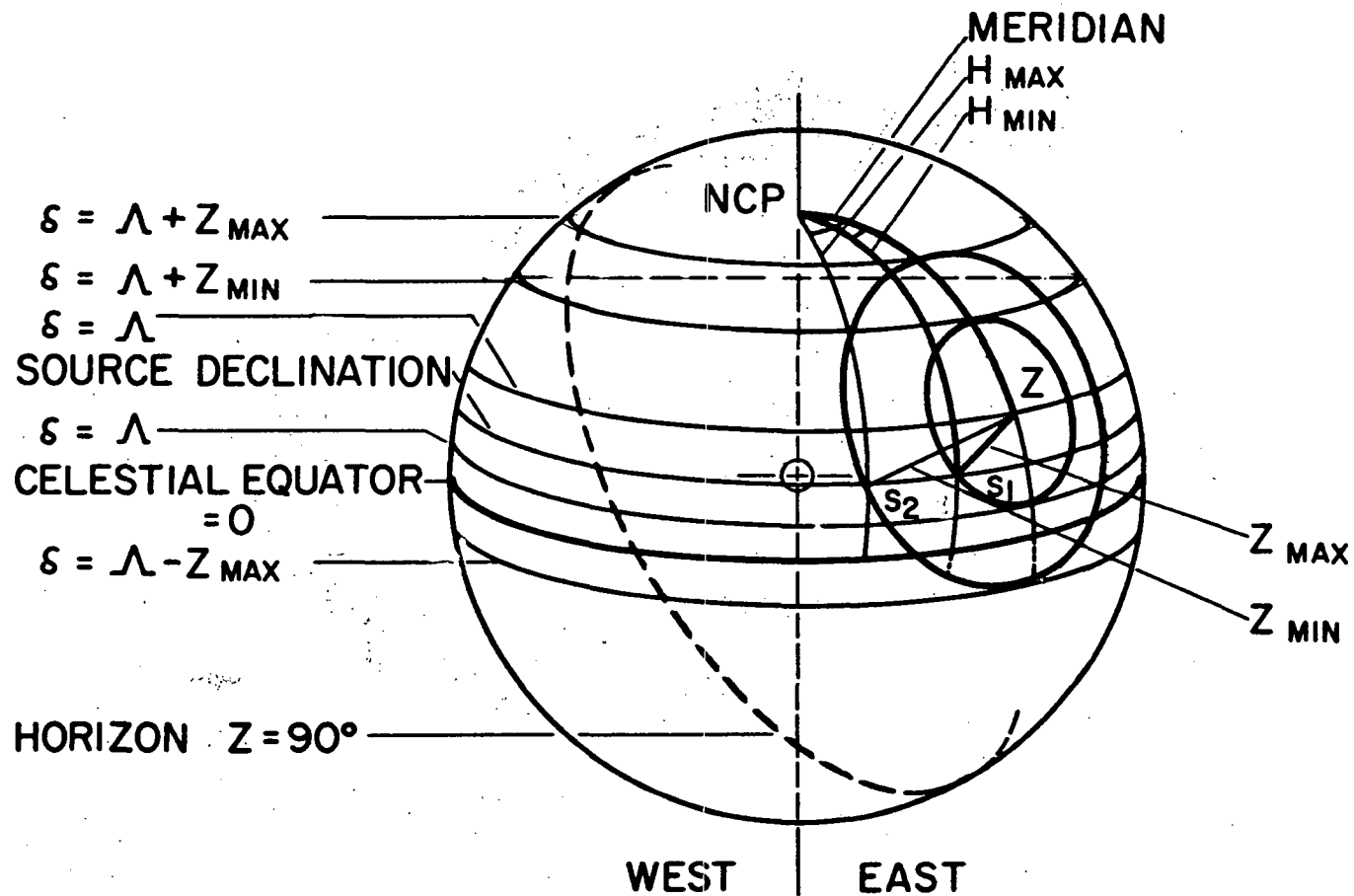
Figure 3.1

Geometry on the celestial sphere for the hour angle function $\Delta H = H_{MAX} - H_{MIN}$ for an observer centered on O at latitude Λ. ΔH gives the time (hour angle) for a source to move from position S_1 on one almucantar to position S_2 on another, neglecting atmospheric refraction.
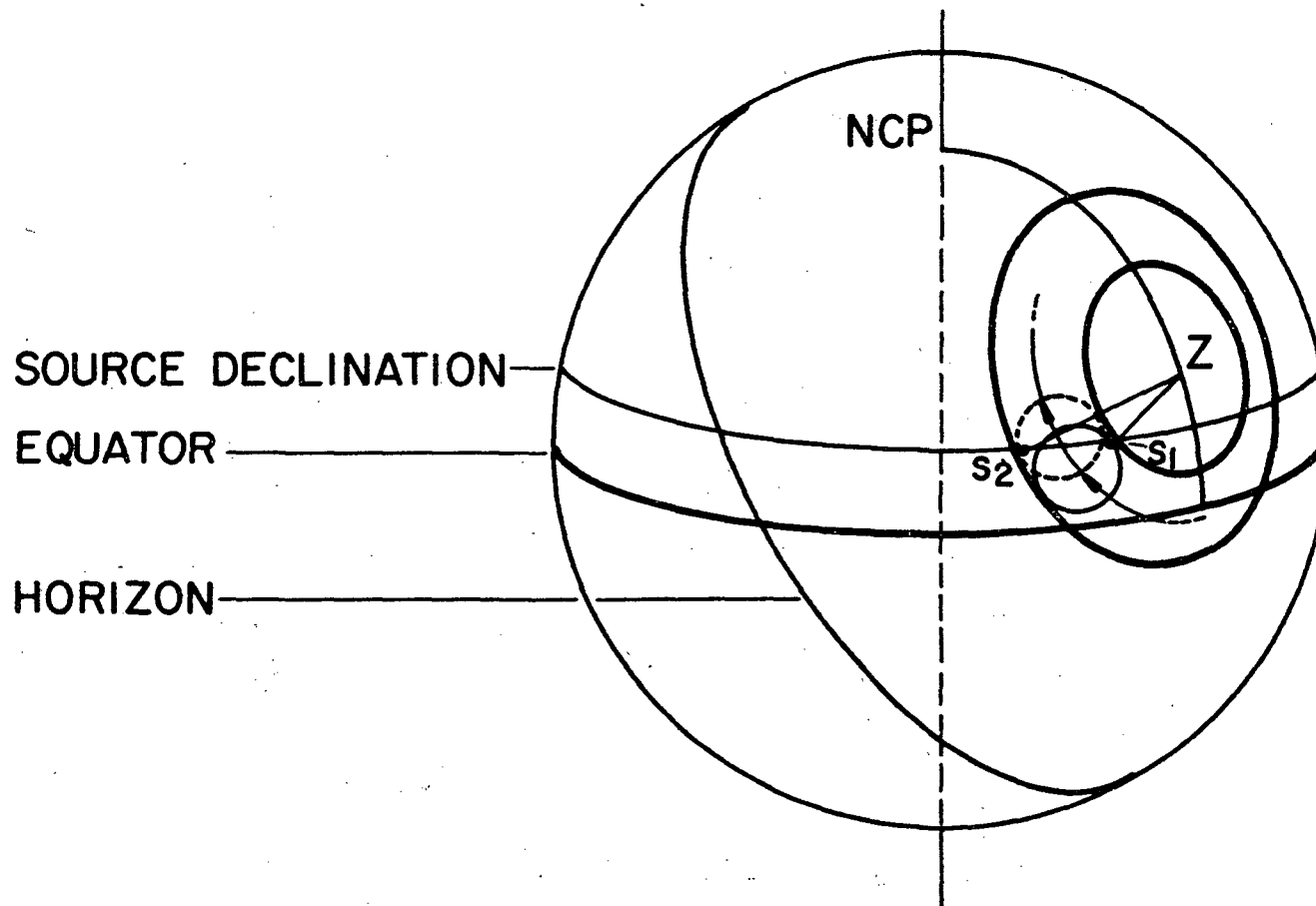
Figure 3.2

As in Figure 3.1, for azimuthal tracking
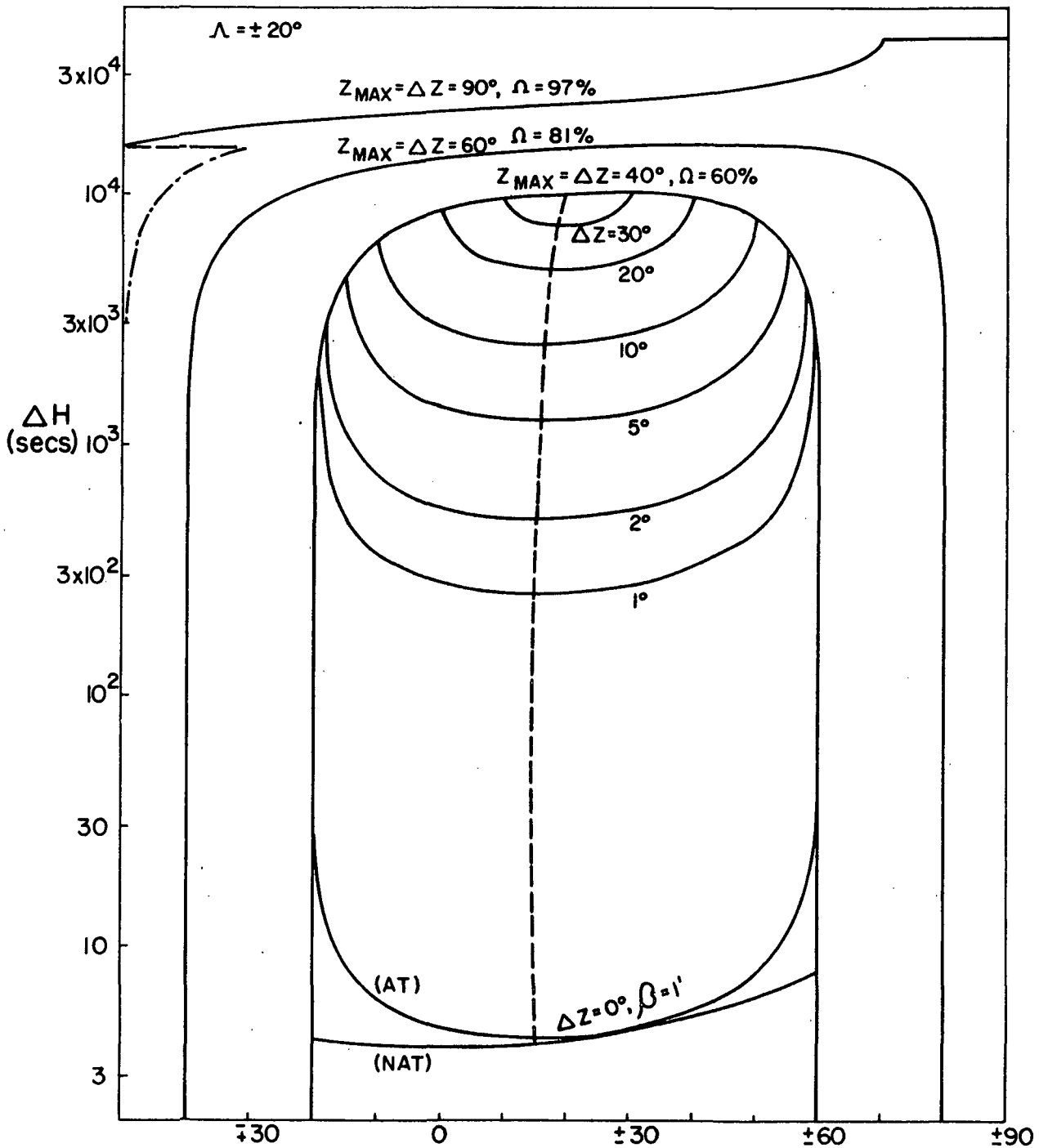with a finite half power beam width 2χ.

Figure 3.3a

Time ΔH (seconds) for which a point source is accessible under parametric conditions on Z_{MAX} and ΔZ stated on the graph. Ω gives the percentage solid angle of the sky accessible. AT and NAT in the case ΔZ = 0 refer to azimuthal tracking and no azimuthal tracking (i.e. pure transit) telescopes for HPBW β = 1 arc minute. Average values for ΔH are given in Table 3.1.
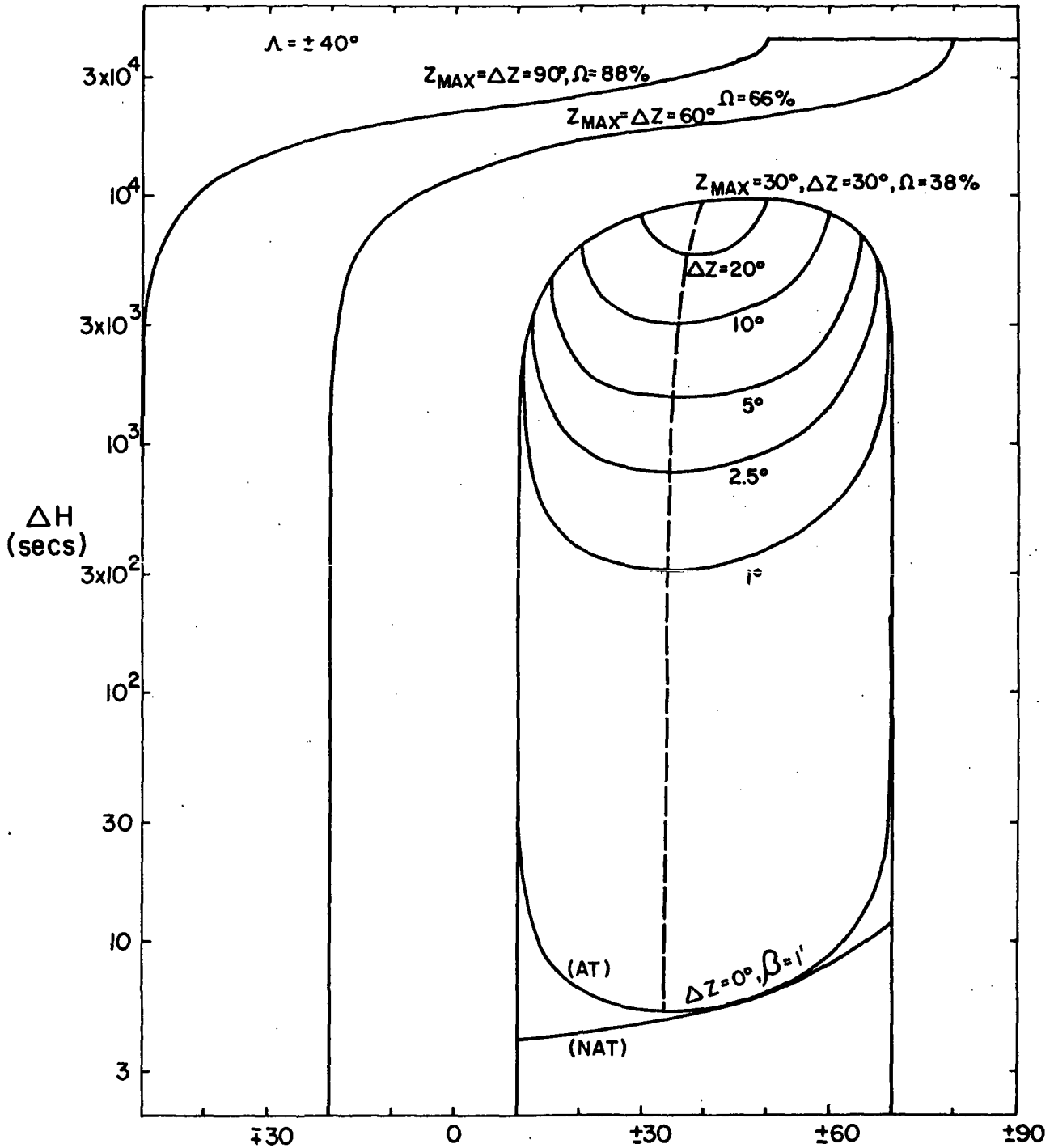
Figure 3.3b
Time ΔH (seconds) for which a point source is accessible under parametric conditions on
Z_{MAX} and ΔZ stated on the graph. Ω gives the percentage solid angle of the sky
accessible. AT and NAT in the case ΔZ = 0 refer to azimuthal tracking and no azimuthal
tracking (i.e. pure transit) telescopes for HPBW β = 1 arc minute. Average values for
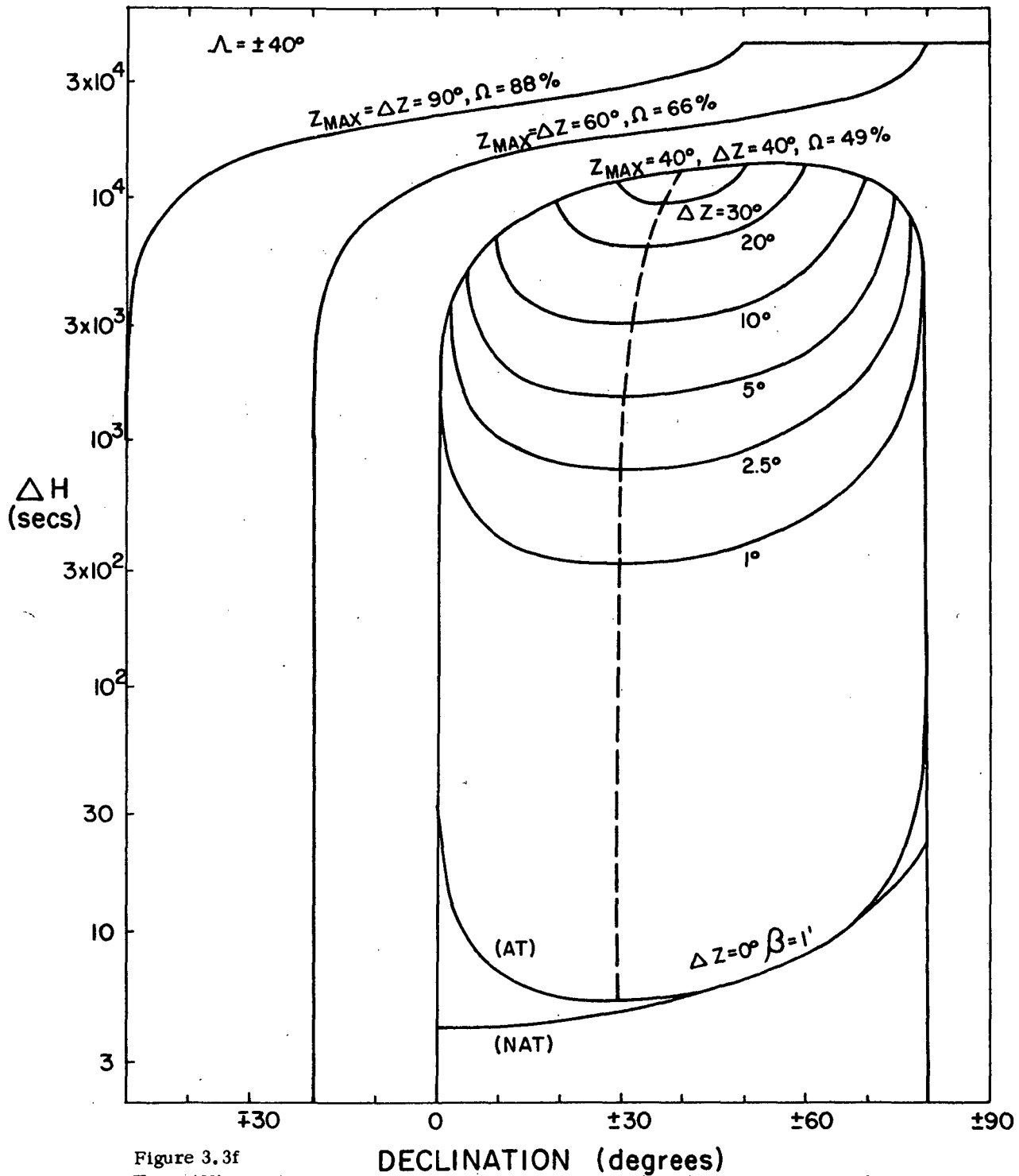ΔH are given in Table 3.1.
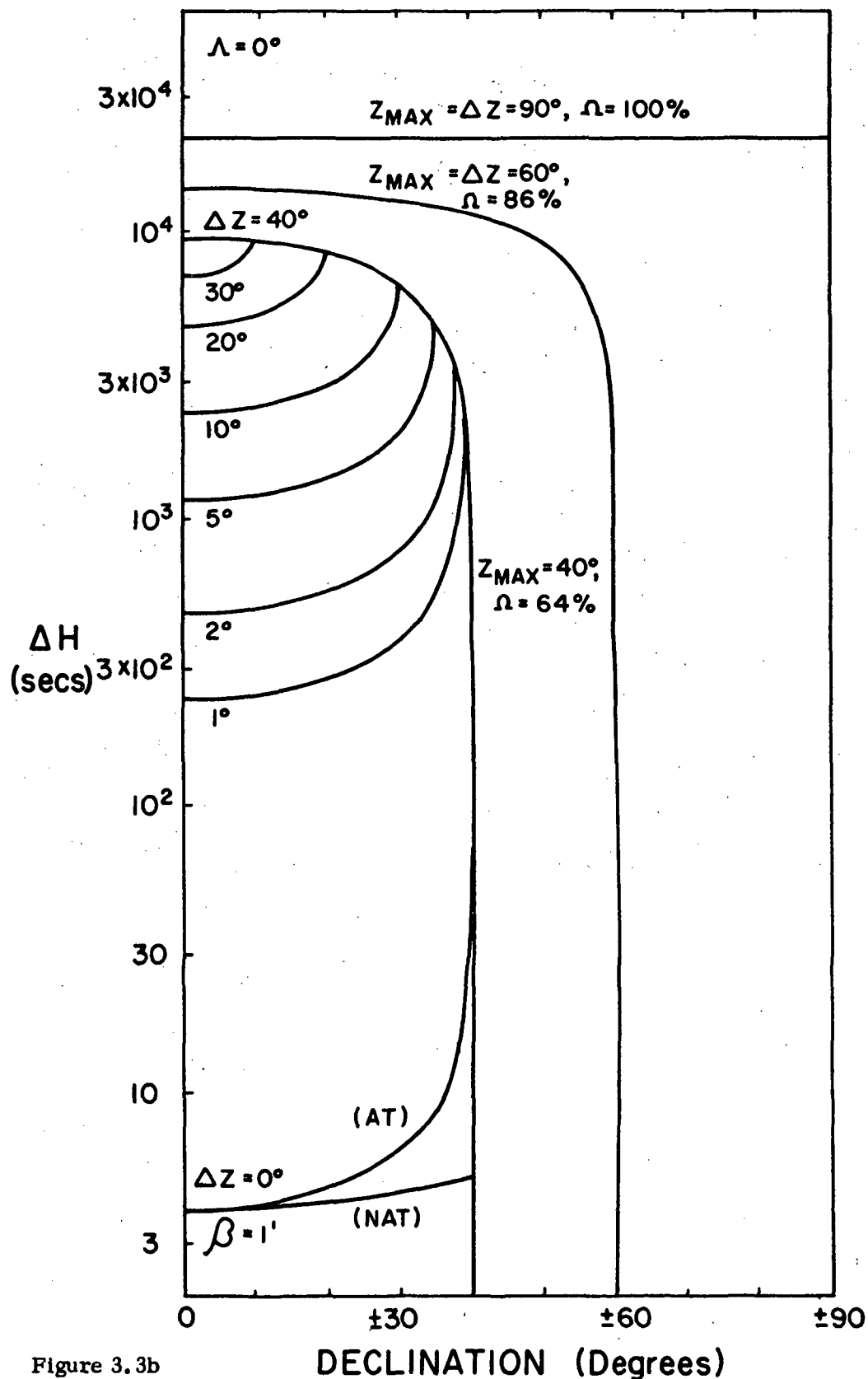
Figure 3.3c
Time ΔH (seconds) for which a point source is accessible under parametric conditions on Z_{MAX} and ΔZ stated on the graph. Ω gives the percentage solid angle of the sky accessible. AT and NAT in the case $\Delta Z = 0$ refer to azimuthal tracking and no azimuthal tracking (i.e. pure transit) telescopes for HPBW $\beta = 1$ arc minute. Average values for ΔH are given in Table 3.1.

Figure 3.3d DECLINATION (DEGREES)

Time ΔH (seconds) for which a point source is accessible under parametric conditions on Z_{MAX} and ΔZ stated on the graph. Ω gives the percentage solid angle of the sky accessible. AT and NAT in the case ΔZ = 0 refer to azimuthal tracking and no azimuthal tracking (i.e. pure transit) telescopes for HPBW β = 1 arc minute. Average values for ΔH are given in Table 3.1.
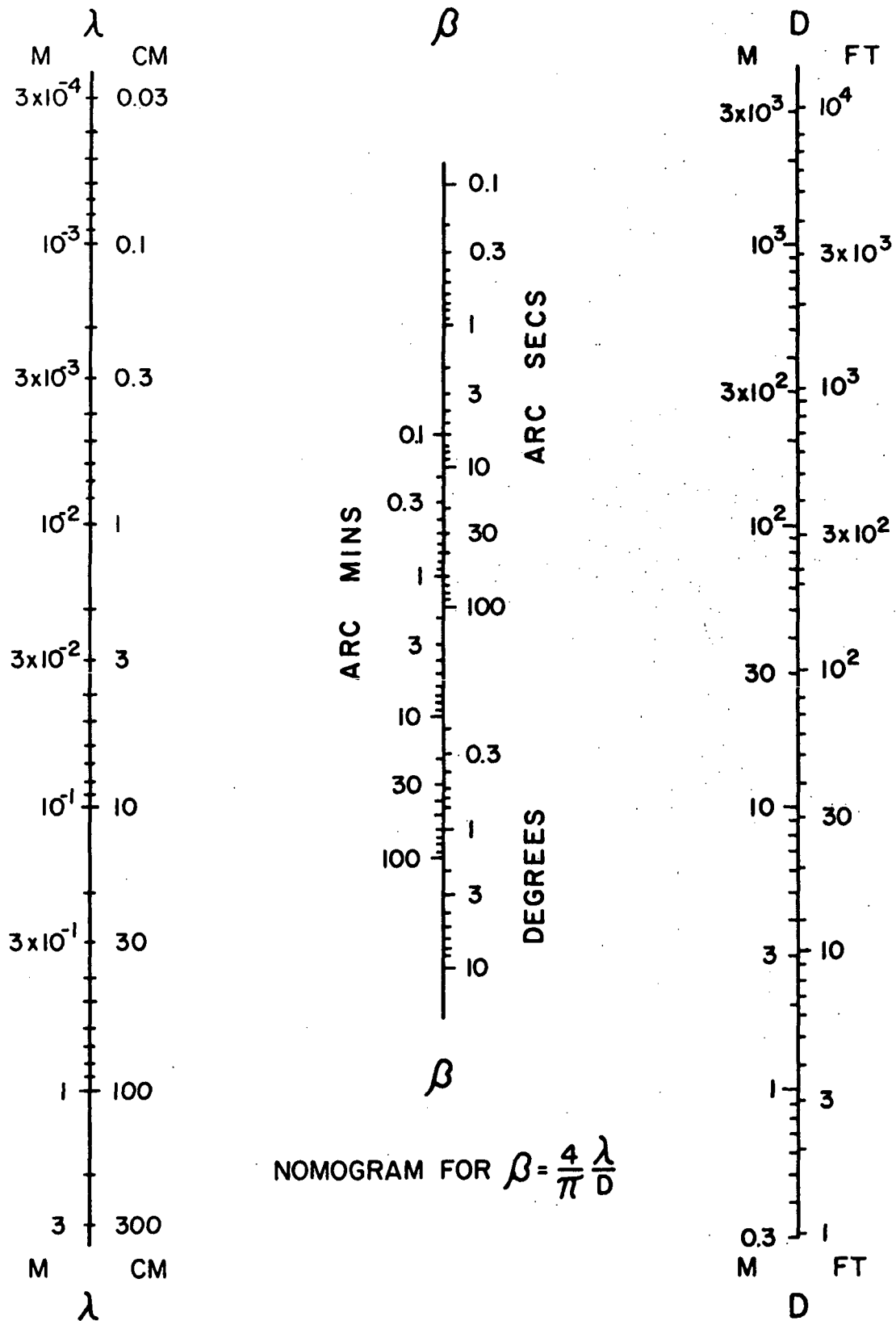
Figure 3.3e

DECLINATION δ

Time ΔH(seconds) for which a point source is accessible under parametric conditions on Z_{MAX} and ΔZ stated on the graph. Ω gives the percentage solid angle of the sky accessible. AT and NAT in the case $\Delta Z = 0$ refer to azimuthal tracking and no azimuthal tracking (i.e. pure transit) telescopes for HPBW $\beta = 1$ arc minute. Average values for ΔH are given in Table 3.1.

Figure 3.3f

Time ΔH(seconds) for which a point source is accessible under parametric conditions on Z_{MAX} and ΔZ stated on the graph. Ω gives the percentage solid angle of the sky accessible. AT and NAT in the case $\Delta Z = 0$ refer to azimuthal tracking and no azimuthal tracking (i.e. pure transit) telescopes for HPBW $\beta = 1$ arc minute. Average values for ΔH are given in Table 3.1.
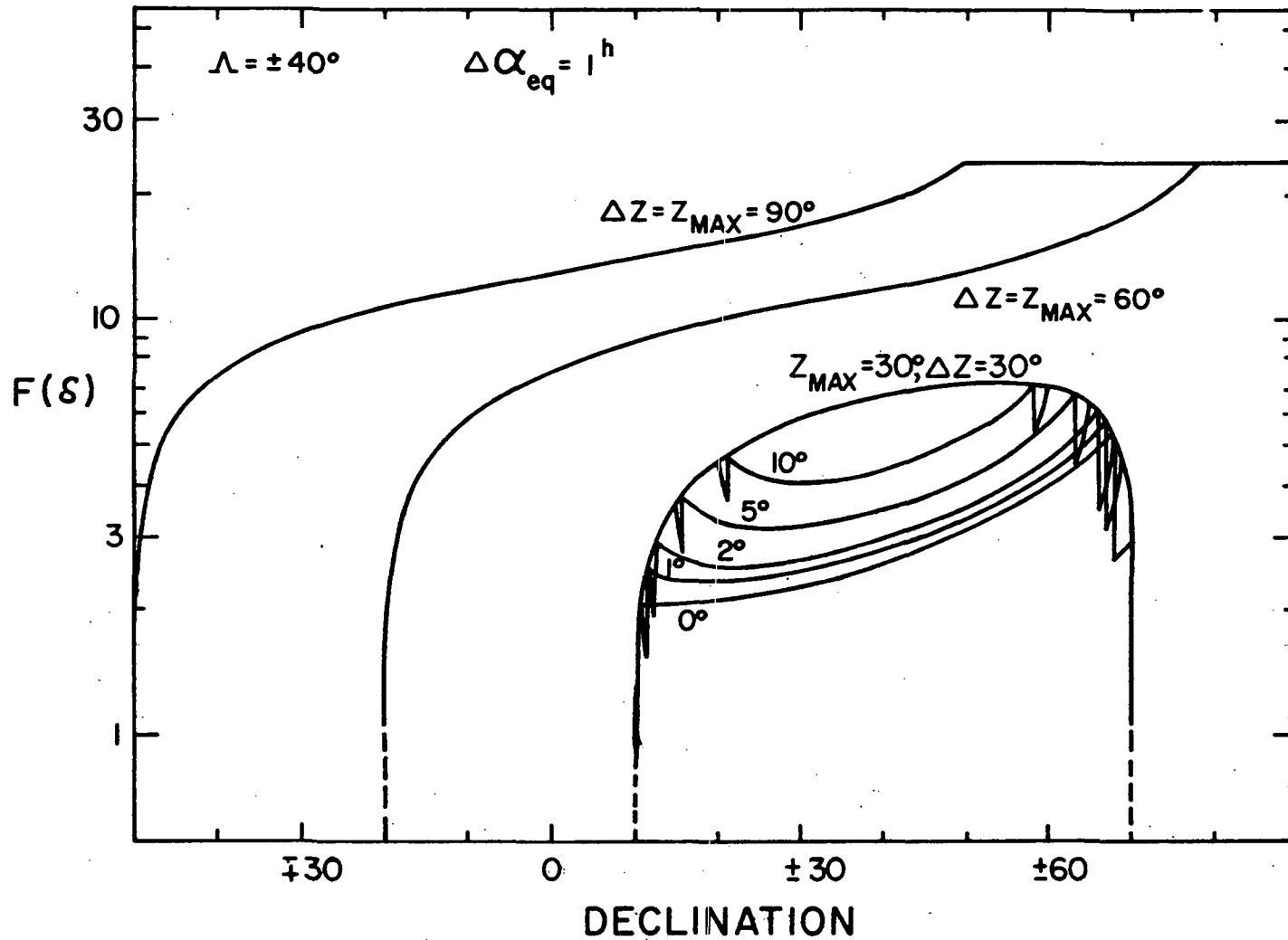
Figure 3.4

Nomogram for $\beta = 4\lambda/\pi D$.
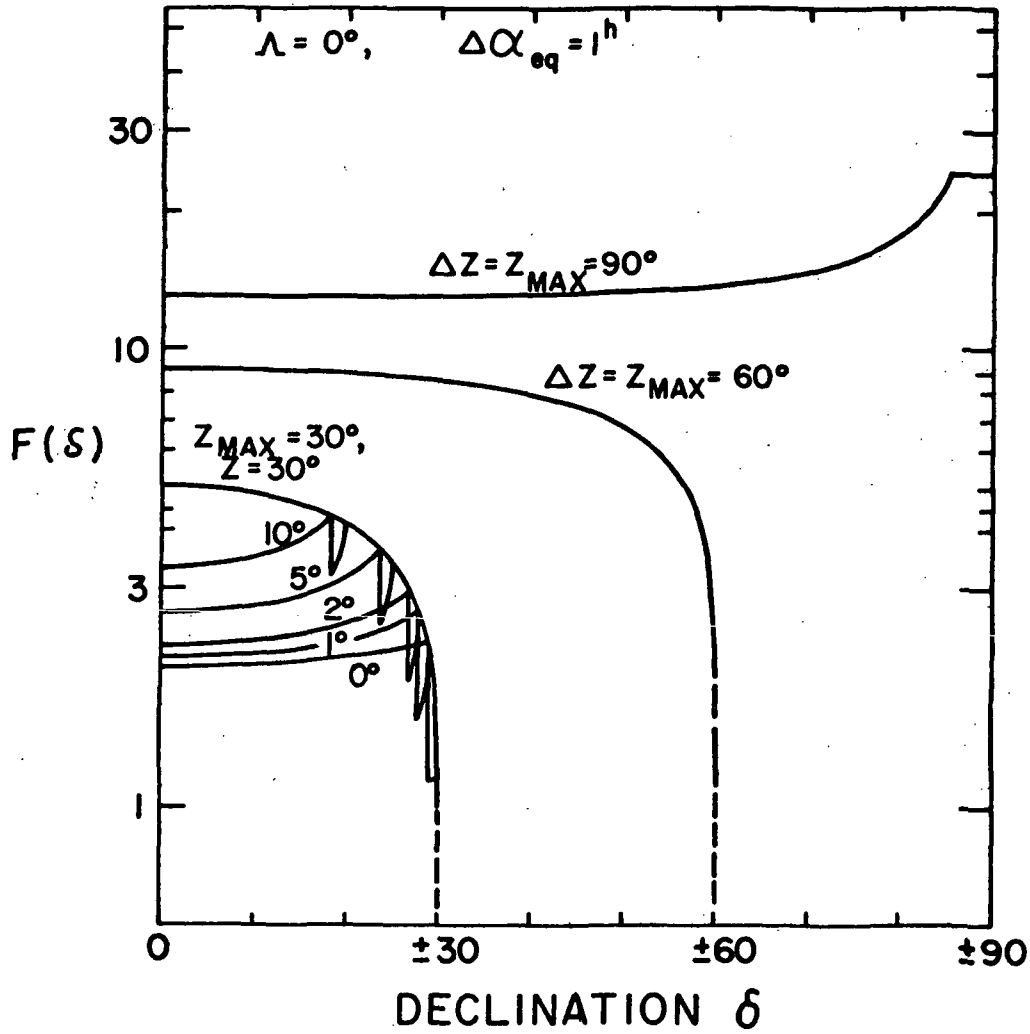
Figure 4.1a

The integration time $F(\delta)$ per day per unit half power beamwidth for a point source in a range of right ascension $\Delta\alpha = \Delta\alpha_{eq}$ sec δ under the conditions indicated on the graph, where $F(\delta)$ is calculated according to Equation (4.9).
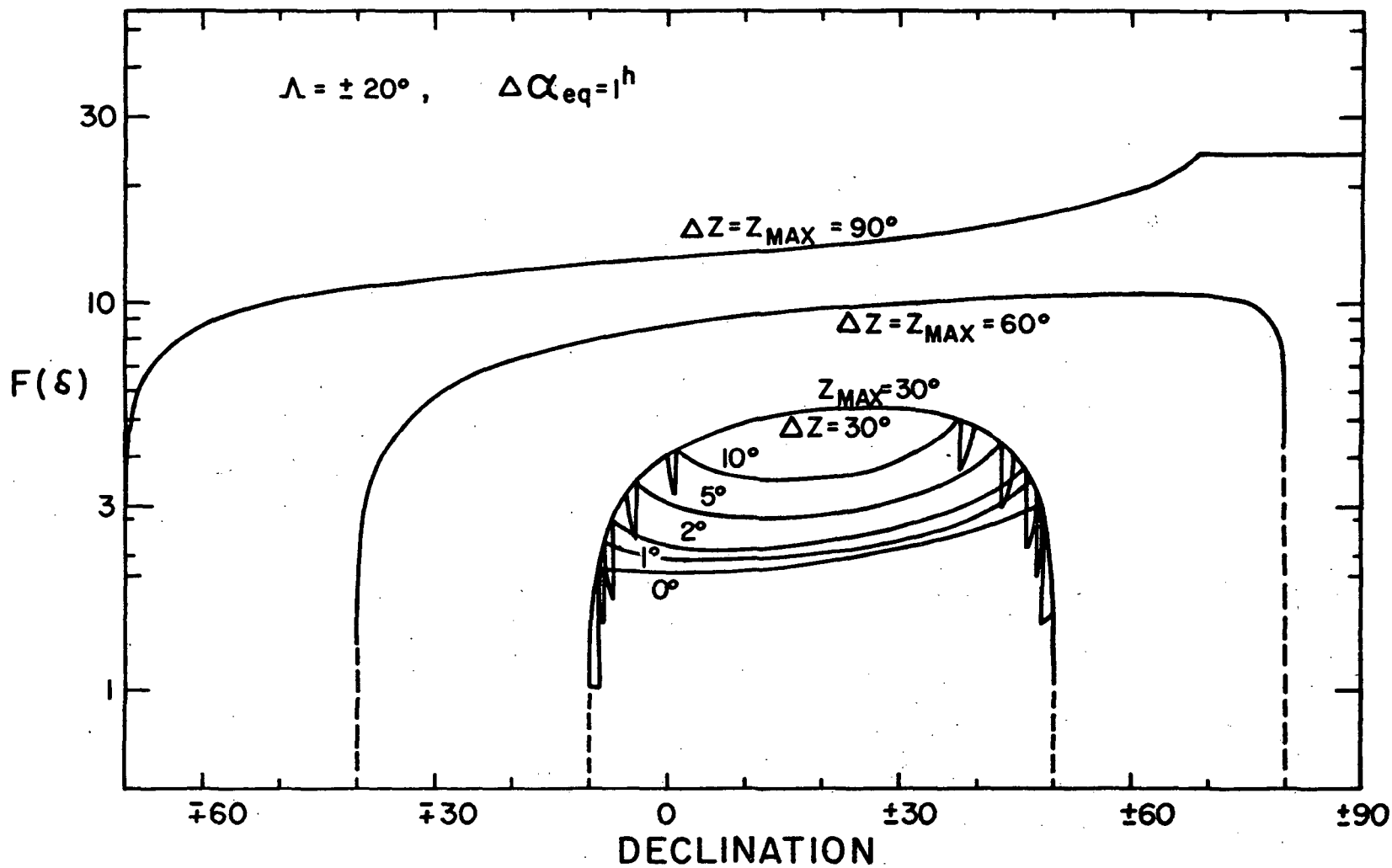
Figure 4. 1b

The integration time F(δ) per day per unit half power beamwidth for a point source in a range of right ascension $\Delta\alpha = \Delta\alpha_{eq}$ sec δ under the conditions indicated on the graph, where F(δ) is calculated according to Equation (4.9).

Figure 4.1c

The integration time F(δ) per day per unit half power beamwidth for a point source in a range of right ascension $\Delta\alpha = \Delta\alpha_{eq}$ sec δ under the conditions indicated on the graph, where F(δ) is calculated according to Equation (4.9).
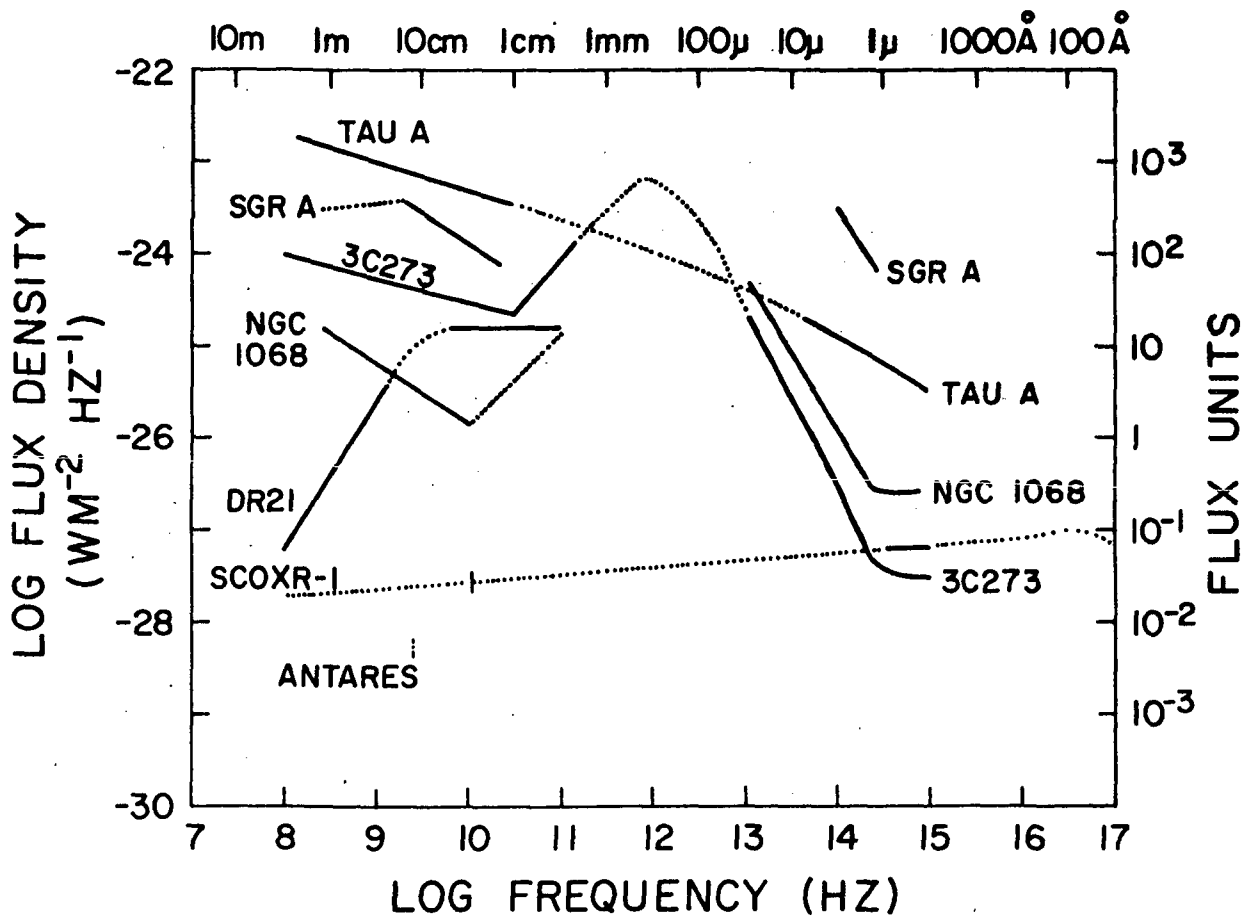
Figure 5.1

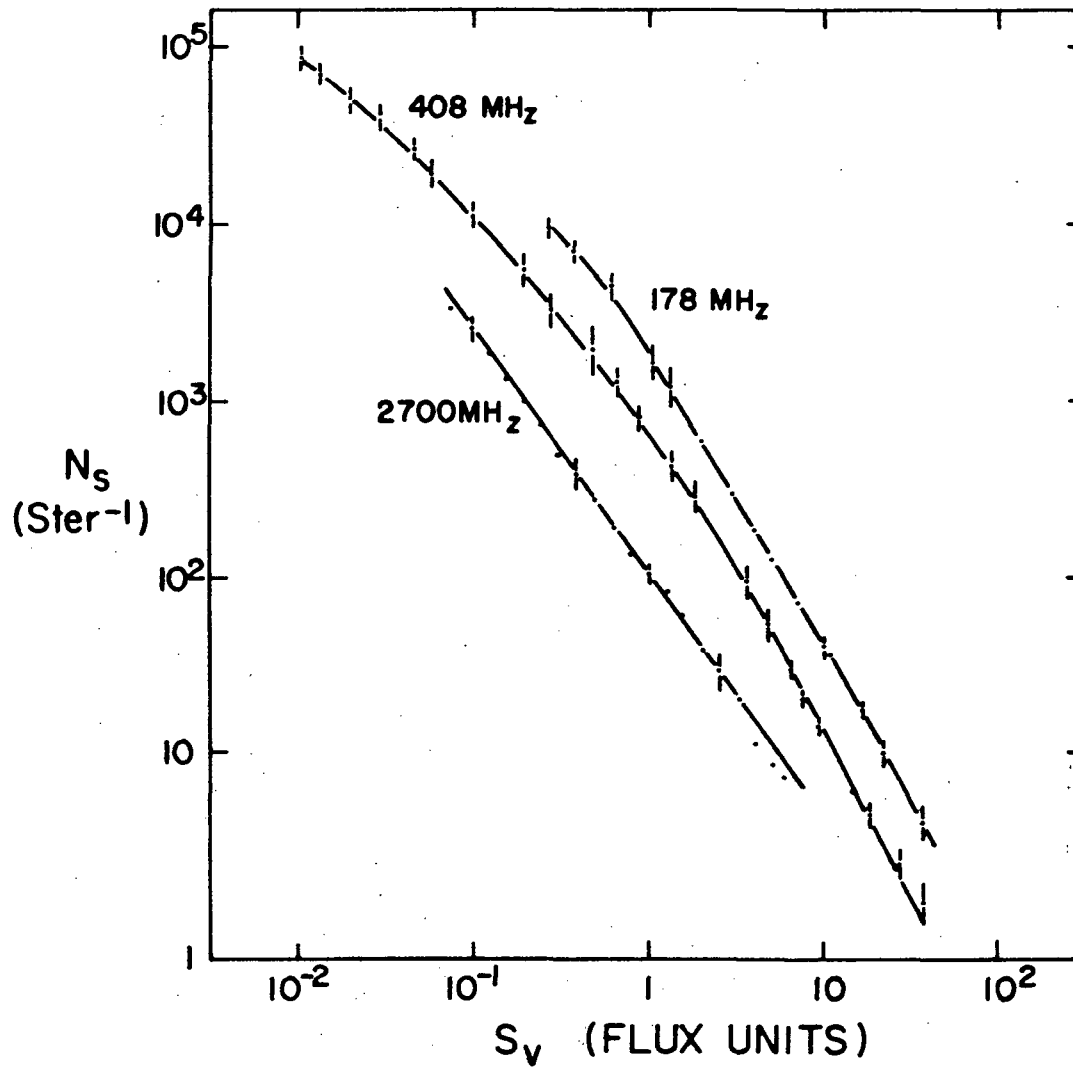Continuum power spectrum for selected sources. Dotted lines are surmised or interpolated.

Figure 5.2

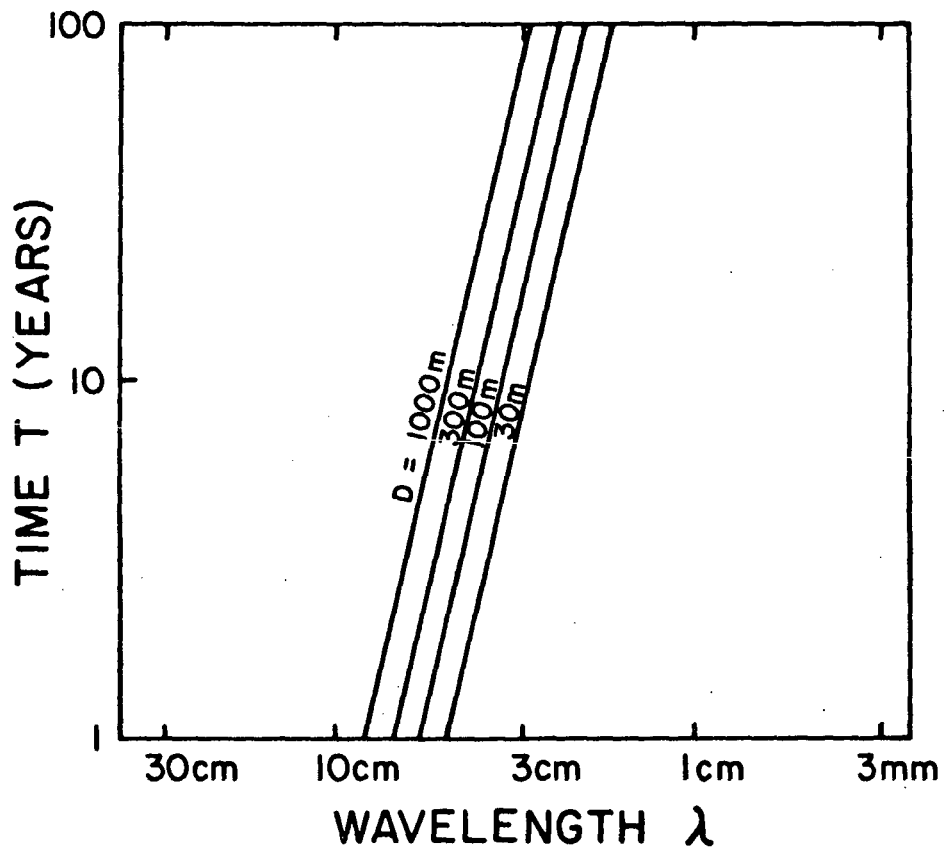An approximate representation of source counts at 178 MHz, 408 MHz and 2700 MHz.

Figure 5.3

Observing time T in years versus wavelength as a function
of various dish sizes, for which confusion and sensitivity limited
operation hold simultaneously for source counting over an area
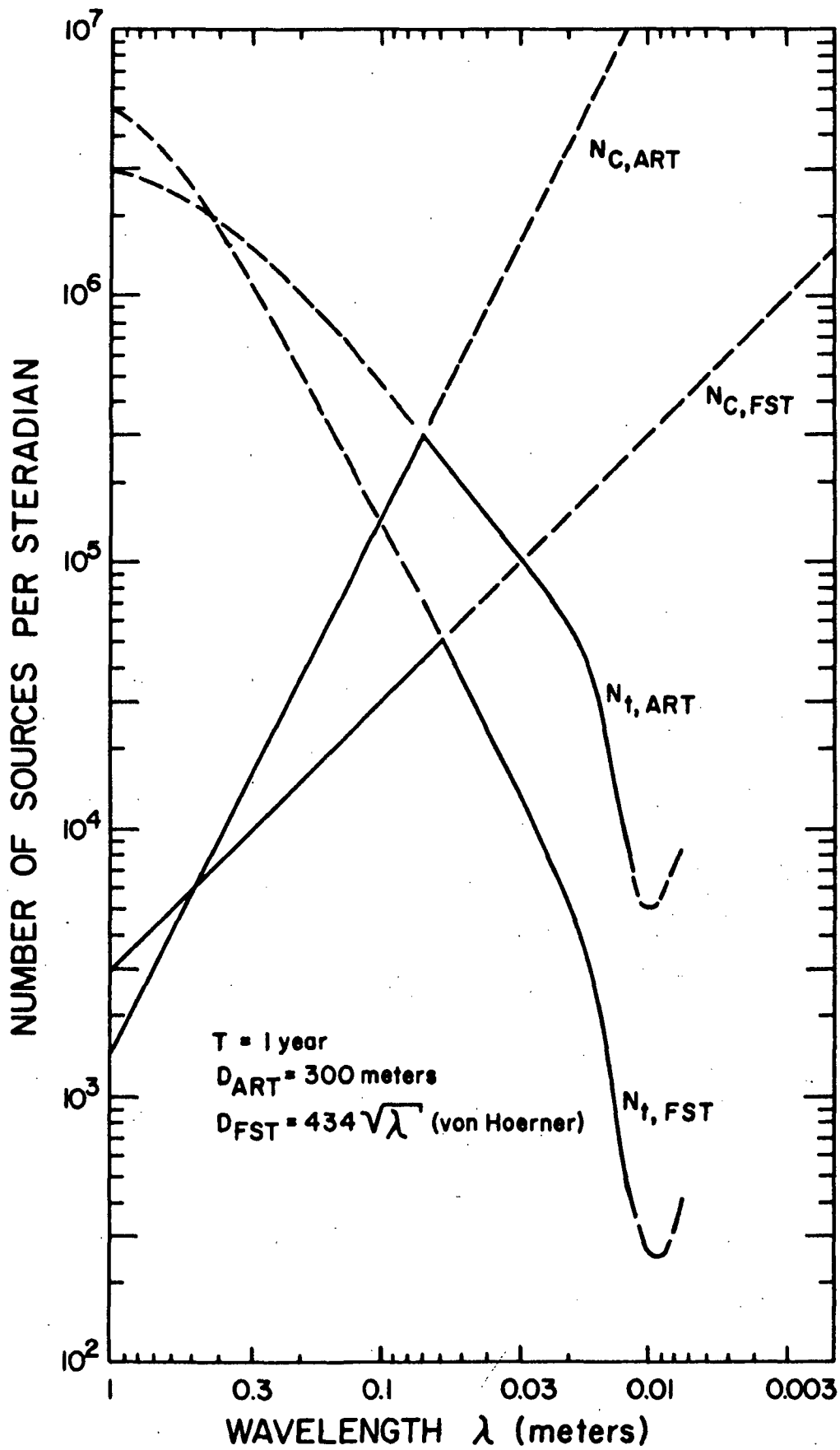of the sky of 4.87λ steradians where $0.3m \gtrsim \lambda \gtrsim 0.01$ m.

Figure 5.4

Figure 5.4

The number of sources per steradian limited by confusion (N_C) and by an observing time of 1 year (N_t) for an almucantar radio telescope (ART) of diameter 300 meters and a largest feasible fully steerable telescope (FST) with diameter estimated from an equation of von Hoerner (1967). Maser capabilities are assumed and total noise temperatures are given in Table 5.1. The observed solid angle of sky is 4.87 λ steradians, $0.01 \gtrsim \lambda \gtrsim 0.3$. The point of intersection of the N_C and N_t curves agrees with the value given by Figure 5.3. The function N_t assumes a homogeneous Euclidean universe with mean spectral index of sources of $\alpha = 0.75$ and slope for the log N-log S function of -1.5, which has been normalized to the data of Shimmins, Bolton and Wall (1968). Cosmological model discrimination can occur for $N(\text{ster}^{-1}) \gtrsim 10^4$ sources. For project times that are a factor f greater than one year, the N_t family of curves must be displaced upward (or downward) by a factor $f^{3/4}$, or 5.6 for $f = 10$.

Results show that almucantar telescopes outperform fully steerable ones in the source counting problem for all $\lambda \lesssim 50$ cm, by ever increasing amounts as λ decreases, for project times of 1 year or greater.
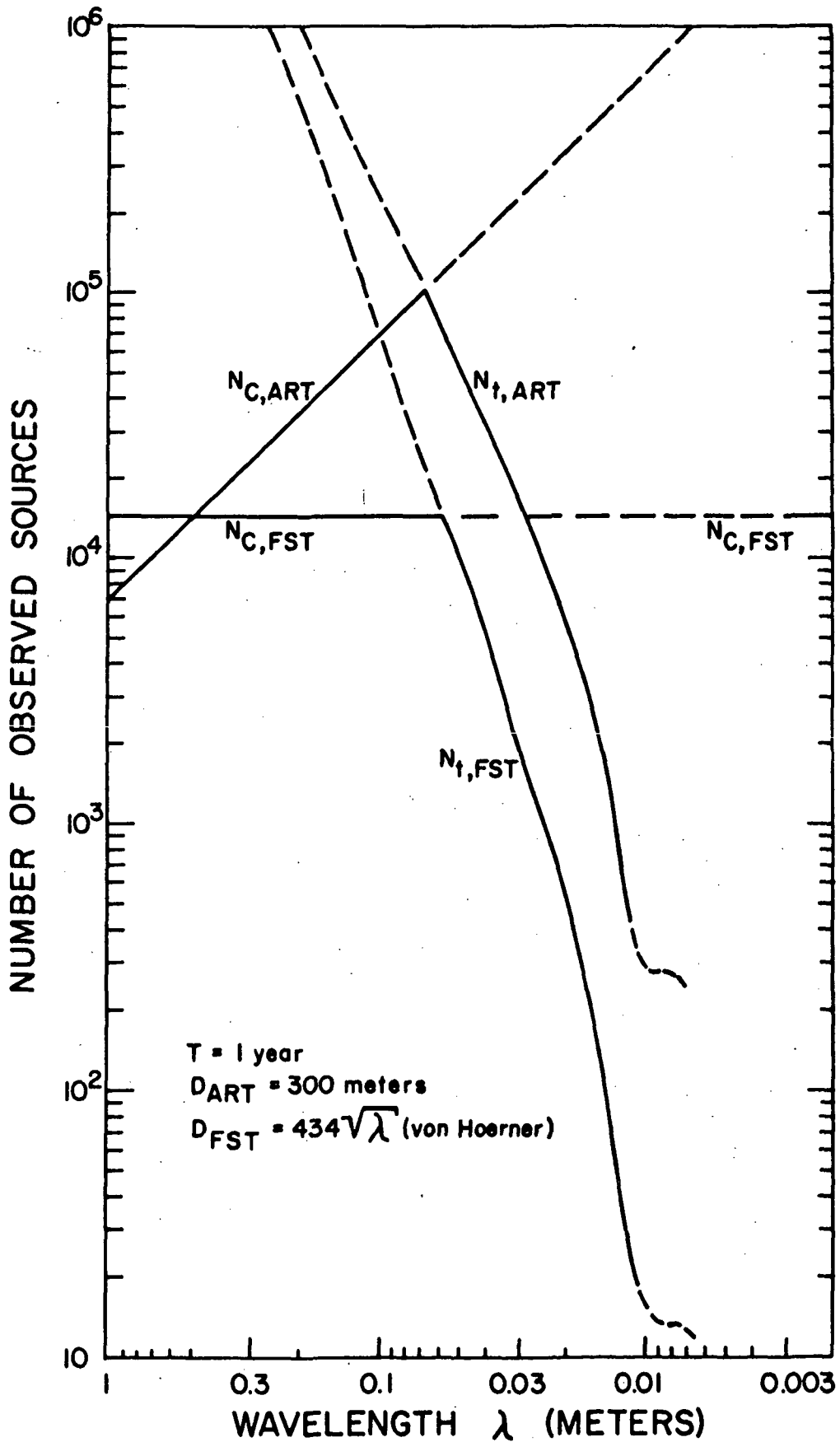
Figure 5.5
The number of observed sources for the particular model described
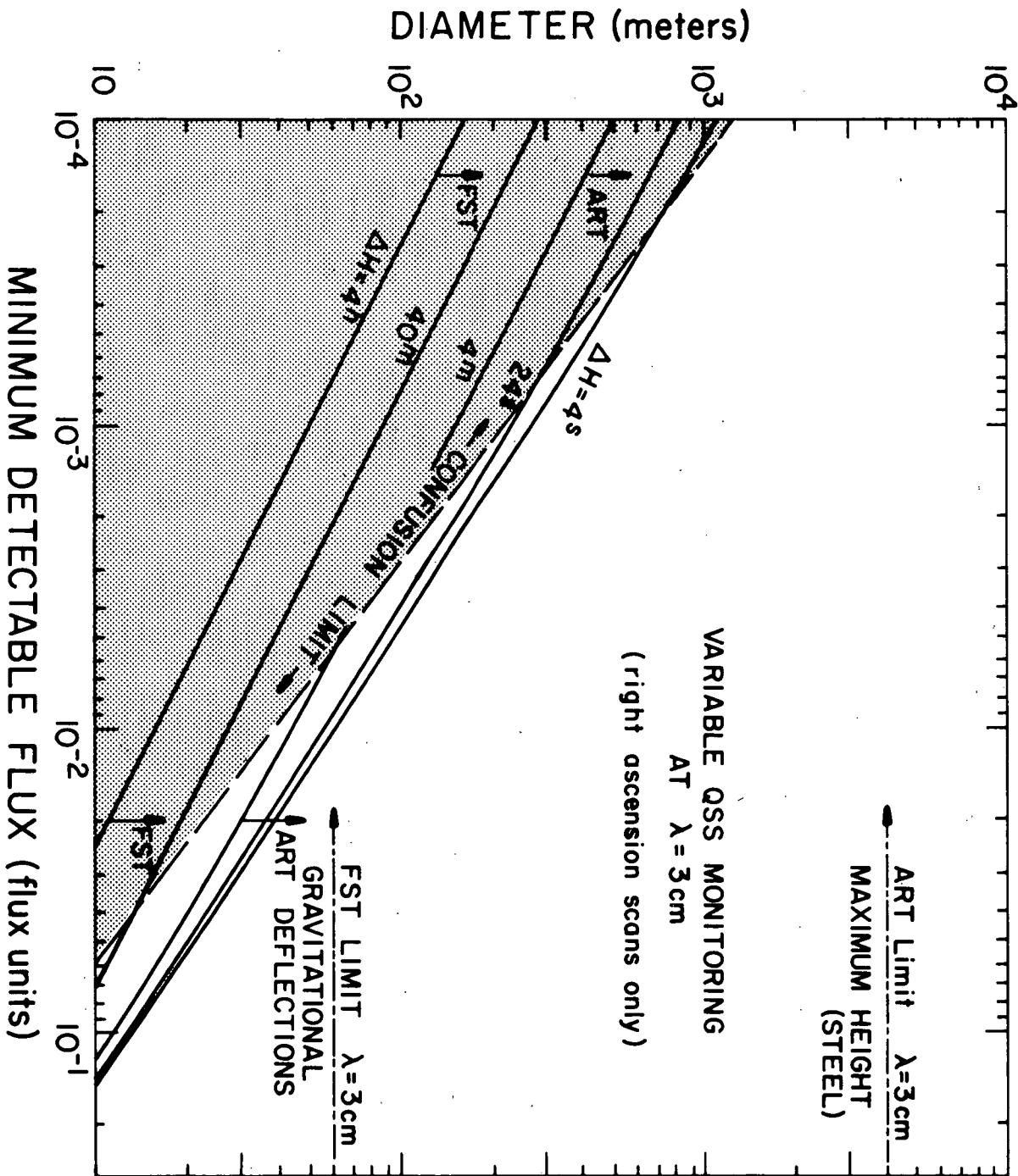in the text and conditions pertaining to Figure 5.4.

DIAMETER (meters)

10^4

10^3

10^2

10

10^{-4} 10^{-3} 10^{-2} 10^{-1}

MINIMUM DETECTABLE FLUX (flux units)

$\Delta H = 4^h$

40^m

FST

ART

4^m

24^s

CONFUSION LIMIT

$\Delta H = 4^s$

FST

FST

ART

$\underline{ART~Limit~~\lambda = 3cm}$
MAXIMUM HEIGHT
(STEEL)

VARIABLE QSS MONITORING
AT $\lambda = 3$ cm
(right ascension scans only)

FST LIMIT $\lambda = 3$ cm
GRAVITATIONAL
ART DEFLECTIONS

Figure 5. 6

Minimum detectable flux as a function of dish diameter for right ascension scans of about
8 half-power beamwidths at a wavelength of 3 cm, for durations of observation of
$2\Delta H$ per day. The confusion limit is shown as well as von Hoerner's value for the
largest feasible fully steerable dish at 3 cm. Curves with $\Delta H < 4^h$ are applicable to
fully steerable dishes operating up to maximum zenith angles of 60°; curves with
$\Delta H \leq 4^m$ are applicable to almucantar telescopes with $\Delta Z = 1°$. The much larger
dish sizes realizable by the almucantar design clearly overcome any advantage that
accrues from full steerability.